

Supplementary Information

Ru(II)-dmso Complexes containing Azole-based Ligands: Synthesis, Linkage Isomerism and Catalytic Behaviour

Íngrid Ferrer, Xavier Fontrodona, Montserrat Rodríguez* and Isabel Romero*

Departament de Química and Serveis Tècnics de Recerca, Universitat de Girona, Campus de Montilivi, E-17071 Girona, Spain.

Keywords: ruthenium /dmso complexes/ azole-based ligands / linkage isomerism / hydration catalysis.

Table of Contents

Table S1. Crystallographic data for complexes **2–5** and **6'**.

Table S2. Formulas used for the calculation of rate (k) and equilibrium (K) constants.

Scheme S1. Ru-dmso complexes gathered in entries 3-6 of Table 2.

Figure S1. NMR spectra of **2**, 400 MHz, CD_2Cl_2 : a) ^1H -NMR; b) ^{13}C -NMR; c) COSY; d) NOESY; e) ^1H - ^{13}C HSQC, f) ^1H - ^{13}C HMBC

Figure S2. NMR spectra of **3**, 300 MHz, CD_2Cl_2 : a) ^1H -NMR; b) ^{13}C -NMR; c) COSY; d) NOESY; e) ^1H - ^{13}C HSQC, f) ^1H - ^{13}C HMBC

Figure S3. NMR spectra of **4**, 300 MHz, CD_2Cl_2 : a) ^1H -NMR; b) ^{13}C -NMR; c) COSY; d) NOESY; e) ^1H - ^{13}C HSQC, f) ^1H - ^{13}C HMBC

Figure S4. NMR spectra of **5**, 300 MHz, CD_2Cl_2 : a) ^1H -NMR; b) ^{13}C -NMR; c) COSY; d) NOESY; e) ^1H - ^{13}C HSQC, f) ^1H - ^{13}C HMBC, g) ^1H -NMR with presence of the minor isomer.

Figure S5. UV-visible spectra of **2** (blue), **3** (green), **4** (grey) and **5** (red) in CH_2Cl_2

Figure S6. CV of a) **3** (blue), **4** (black) and **5** (orange) in $\text{CH}_3\text{CN} + 0.1 \text{ M TBAH}$.

Figure S7. CV registered in CH_2Cl_2 (TBAH, 0.1M) vs Ag/AgCl starting the scanning potential at $E_{\text{init}} = 0.6$ for **2** and 0 V for **6** at scan rates between 0.20 and 8 V/s (equilibration time = 2 s). a) complex **2**, b) complex **6**.

Figure S8. Plot of $i_{\text{C}1}/i_{\text{C}2}$ vs. $1/\nu$ to obtain $K^{\text{III}}_{\text{O-S}}$ for complex **2**.

Figure S9. Plot of $i_{\text{C}1}/i_{\text{C}2}$ vs. $1/\nu$ to obtain $K^{\text{III}}_{\text{O-S}}$ for complex **6**.

Figure S10. Plot of $\nu^{1/2}$ vs. $i_{\text{d}}/i_{\text{k}}$ to obtain $k^{\text{III}}_{\text{S-O}}$ and $k^{\text{III}}_{\text{O-S}}$ for complex **2**.

Figure S11. Plot of $\nu^{1/2}$ vs. $i_{\text{d}}/i_{\text{k}}$ to obtain $k^{\text{III}}_{\text{S-O}}$ and $k^{\text{III}}_{\text{O-S}}$ for complex **6**.

Figure S12. Plot of $\ln(i_{\text{a}1}/\nu^{1/2})$ vs. $1/\nu$ to obtain $k^{\text{II}}_{\text{O-S}}$ for complex **2**.

Figure S13. Plot of $\ln(i_{\text{a}1}/\nu^{1/2})$ vs. $1/\nu$ to obtain $k^{\text{II}}_{\text{O-S}}$ for complex **6**.

Figure S14. NMR spectra of **2** in CD_3CN after irradiation at $t =$ a) 0, b) 45 and c) 90 minutes.

Figure S15. CV of **2** in $\text{CH}_3\text{CN} + 0.1 \text{ M TBAH}$ after irradiation during 90 minutes.

Figure S16. CV of **6'** in $\text{CH}_2\text{Cl}_2 + 0.1 \text{ M TBAH}$.

Figure S17. Successive UV-visible spectra obtained after irradiation of a solution of complex **6** in CHCl_3 during 60 min, to generate complex **6'**.

Figure S18. Successive UV-visible spectra obtained after irradiation of a solution of complex **2** in CHCl_3 during 24 h, to generate complex **2"**.

Figure S19. CV of **2"** in $\text{CH}_2\text{Cl}_2 + 0.1 \text{ M TBAH}$ after irradiation.

Figure S20. UV-vis monitoring of complex **2** in water at 80°C: main figure, spectra registered for 30 minutes; inset, evolution of the band at 516 nm up to 150 minutes.

Figure S21. Red, ^1H -NMR spectrum of complex **2** registered in D_2O . Black, ^1H -NMR spectrum of complex **2** after 150 minutes in water solution at 80°C.

Table S1. Crystallographic data for complexes **2-5** and **6'**.

	2	3	4	5	6'
Empirical formula	C ₁₀ H ₂₄ Cl ₂ N ₂ O ₃ RuS ₃	C ₉ H ₂₁ Cl ₂ N ₃ O ₅ RuS ₃	C ₁₀ H ₂₃ Cl ₂ F ₃ N ₂ O ₄ RuS ₃	C ₁₃ H ₂₄ BrCl ₂ N ₂ O ₄ RuS ₃	C ₁₁ H ₁₅ Cl ₃ N ₃ ORu S
Formula weight	488.46	519.44	560.45	620.40	515.64
Crystal system	Monoclinic	Monoclinic	Monoclinic	Monoclinic	Monoclinic
Space group	P2(1)/c	P21/n	P 21/n	P2(1)/c	P21/c
a [Å]	8.8684(17)	8.396(7)	8.739(3)	12.493(6)	9.969(5)
b [Å]	14.240(3)	15.783(13)	23.299(7)	13.943(7)	16.673(8)
c [Å]	15.809(3)	14.403(12)	10.690(3)	16.522(6)	11.326(6)
α [°]	90	90	90	90	90
β [°]	102.331(3)	105.773(13)	93.393(6)	130.27(2)	96.414 (7)
γ [°]	90	90	90	90	90
V [Å ³]	1950.3(6)	1837(3)	2172.9(12)	2195.9(17)	1870.8(16)
Formula Units/ cell	4	4	4	4	4
Temp. [K]	298(2)	298(2)	298(2)	298(2)	100(2)
ρ _{calc} , [Mg/m ⁻³]	1.664	1.878	1.713	1.877	1.831
μ [mm ⁻¹]	1.407	1.509	1.297	3.083	1.665
Final R indices, [I>2σ(I)]	R1=0.0256 wR2=0.0657	R1=0.0237 wR2=0.0608	R1=0.0390 wR2=0.1193	R1=0.0387 wR2=0.0985	R1 = 0.0400 wR2 = 0.1022
R indices [all data]	R1=0.0298 wR2=0.0681	R1=0.0259 wR2=0.0626	R1=0.0447 wR2=0.1229	R1=0.0523 wR2=0.1052	R1 = 0.0524 wR2 = 0.1111

$$R_1 = \sum ||F_o| - |F_c|| / \sum |F_o|$$

$$wR_2 = [\sum \{w(F_o^2 - F_c^2)^2\} / \sum \{w(F_o^2)^2\}]^{1/2}, \text{ where } w = 1/[\sigma^2(F_o^2) + (0.0042P)^2] \text{ and } P=(F_o^2+2F_c^2)$$

Table S2. Formulas used for the calculation of rate (k) and equilibrium (K) constants.

Equations	Description of parameters
$\frac{i_{c1}}{i_{c2}} = a \cdot \frac{1}{v} + K_{O-S}^{III}$ (eq. 1)	i_c = cathodic peak intensity (A) $a = RT/nF$, with: R = Boltzmann constant (J/(K·mol)) T = temperature (K) n = number of exchanged electrons F = Faraday constant (A·s/mol) v = scan rate (V/s) K = equilibrium constant
$\sqrt{v} = \frac{1}{\frac{0.471}{K_{O-S}^{III}} \cdot \sqrt{\frac{nFl}{RT}}} \cdot \frac{i_d}{i_k} - \frac{1.02}{\frac{0.471}{K_{O-S}^{III}} \cdot \sqrt{\frac{nFl}{RT}}}$ (eq. 2)	i_d = diffusional current in the absence of a chemical reaction ($= i_{a1}$) i_k = measured peak current ($= i_{c1}$) $l = k_{O-S}^{III} + k_{S-O}^{III}$
$K^{II} = K^{III} + e^{\frac{F}{RT} (E_{Ru-S}^0 - E_{Ru-O}^0)}$ (eq. 3)	E^0 = standard potential
$\ln \left(\frac{i_{a1}}{\sqrt{v}} \right) = k_{O-S}^{II} \cdot \frac{1}{v} + b$ (eq. 4)	

Scheme S1. Ru-dmso complexes gathered in entries 3-6 of Table 2.

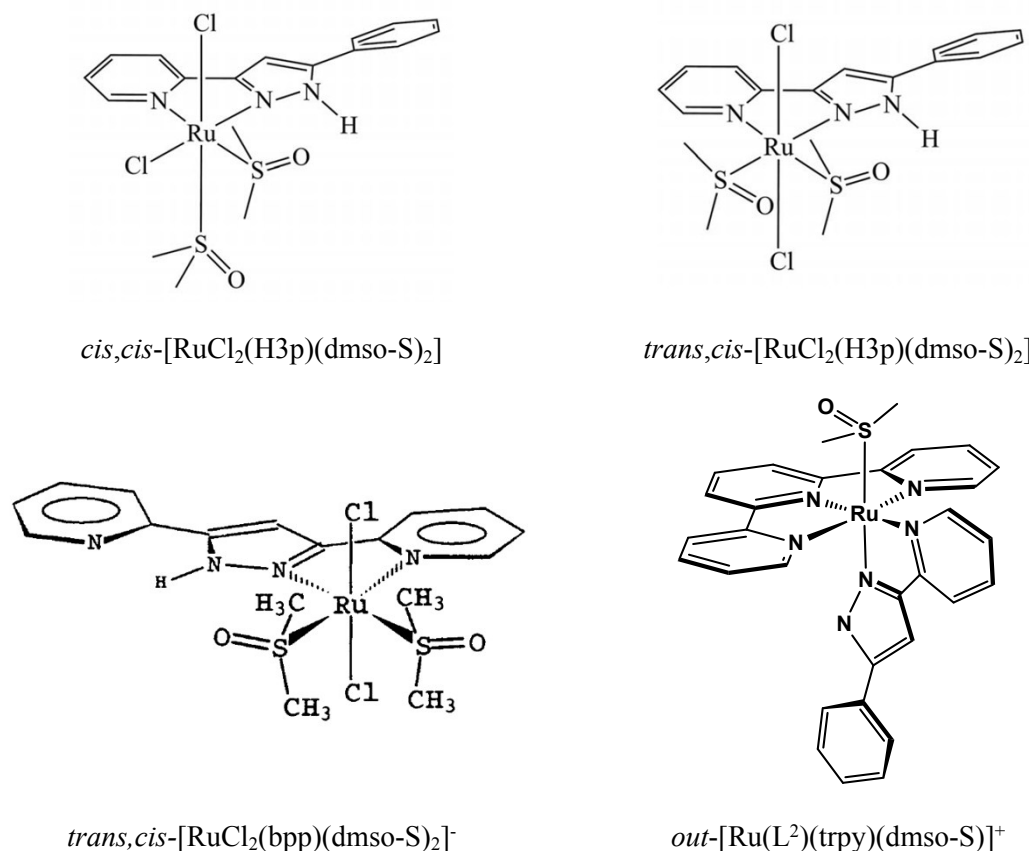
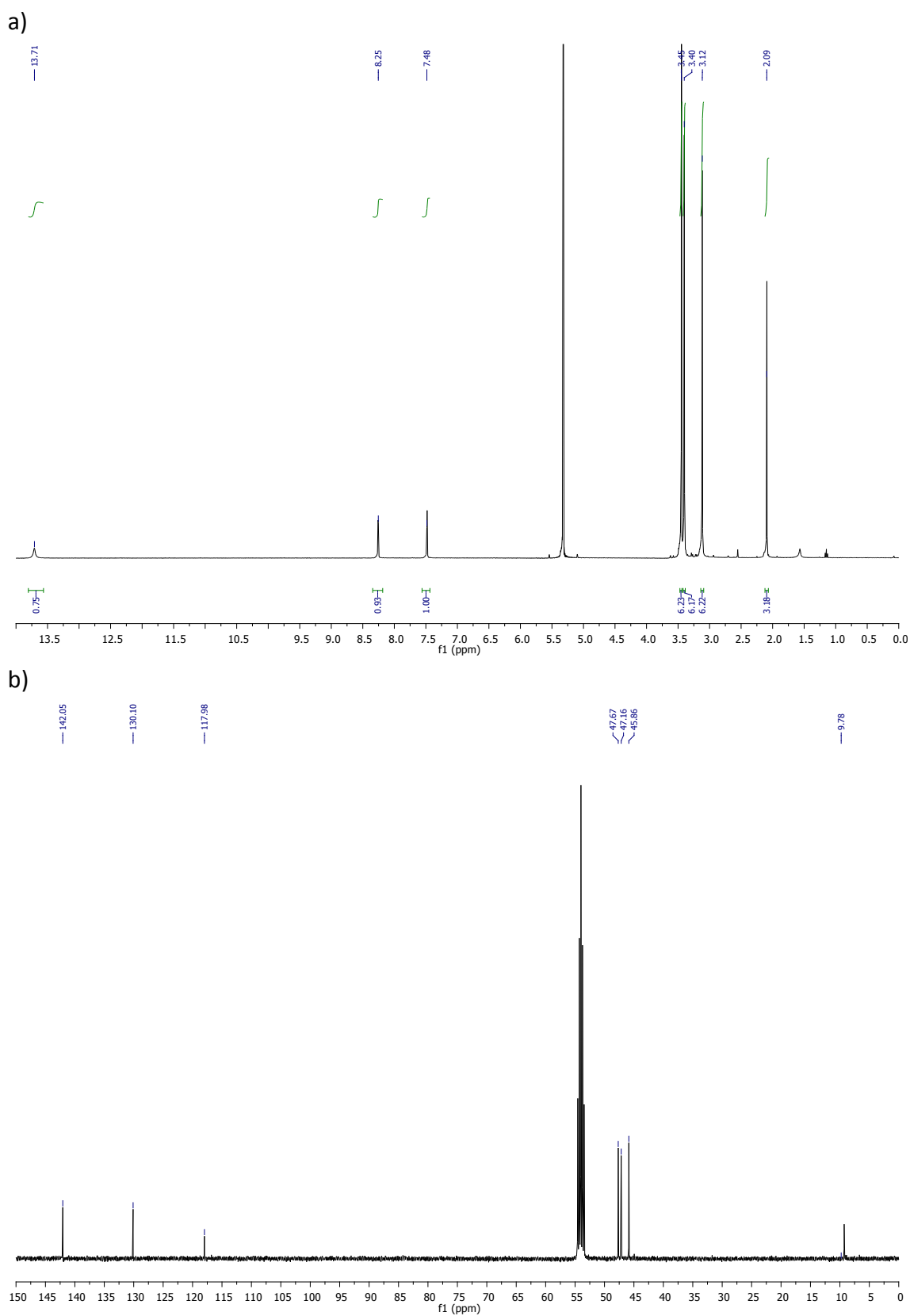
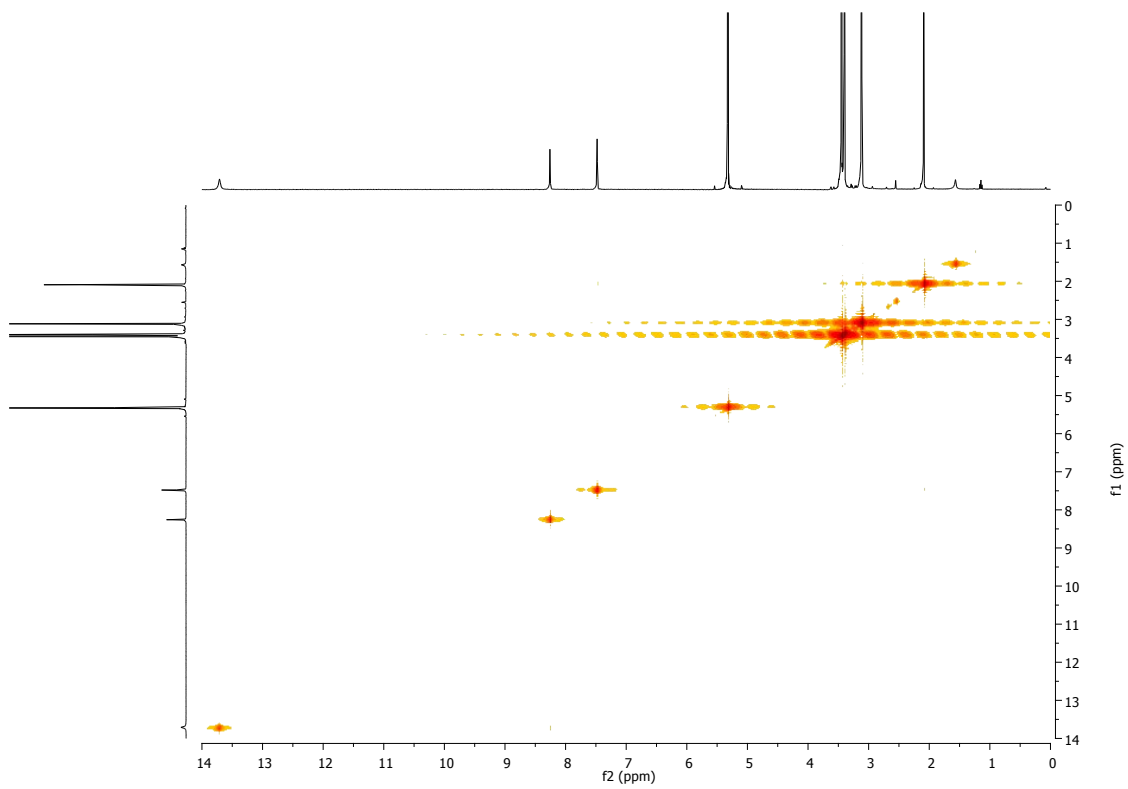


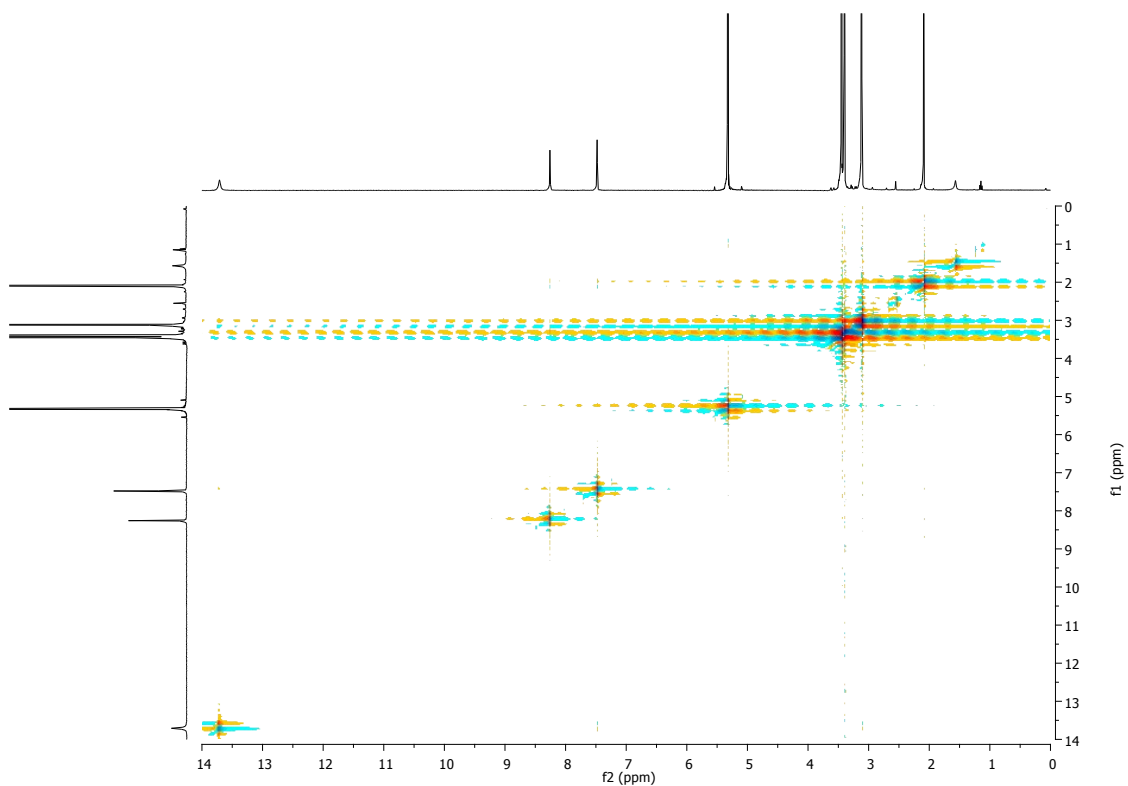
Figure S1. NMR spectra of **2**, 400 MHz, CD₂Cl₂: a) ¹H-NMR; b) ¹³C-NMR; c) COSY; d) NOESY; e) ¹H-¹³C HSQC, f) ¹H-¹³C HMBC



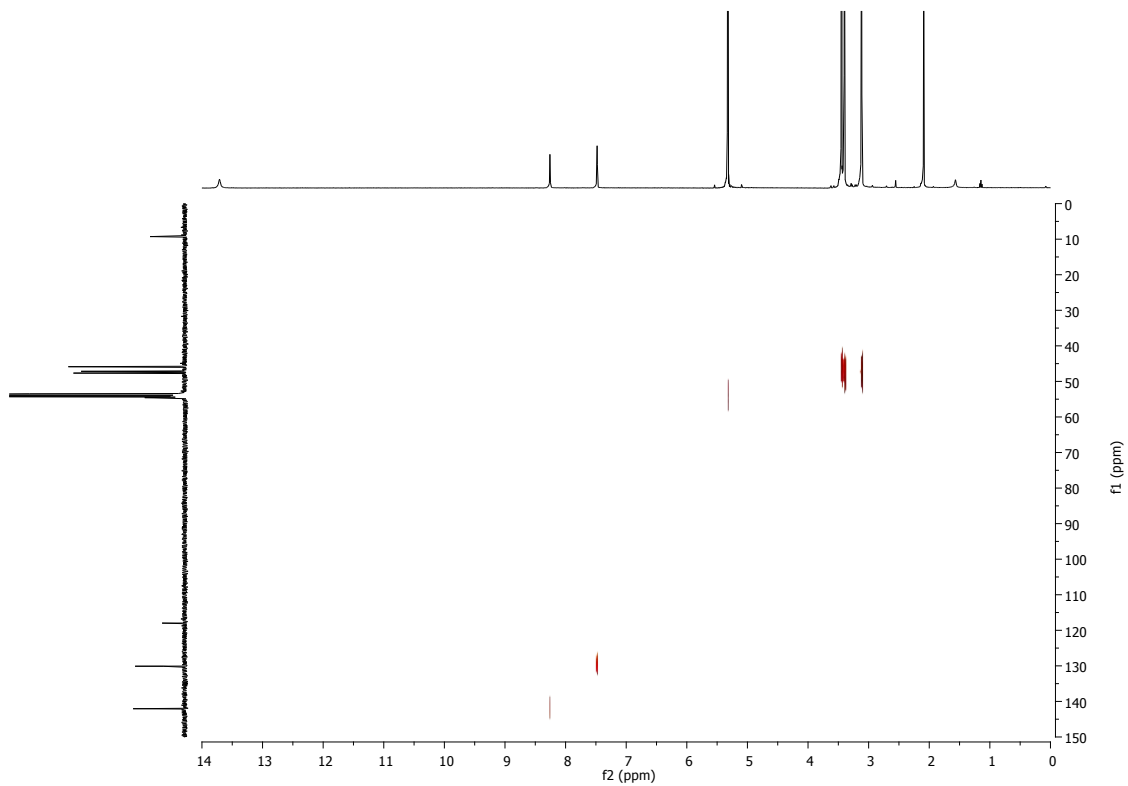
c)



d)



e)



f)

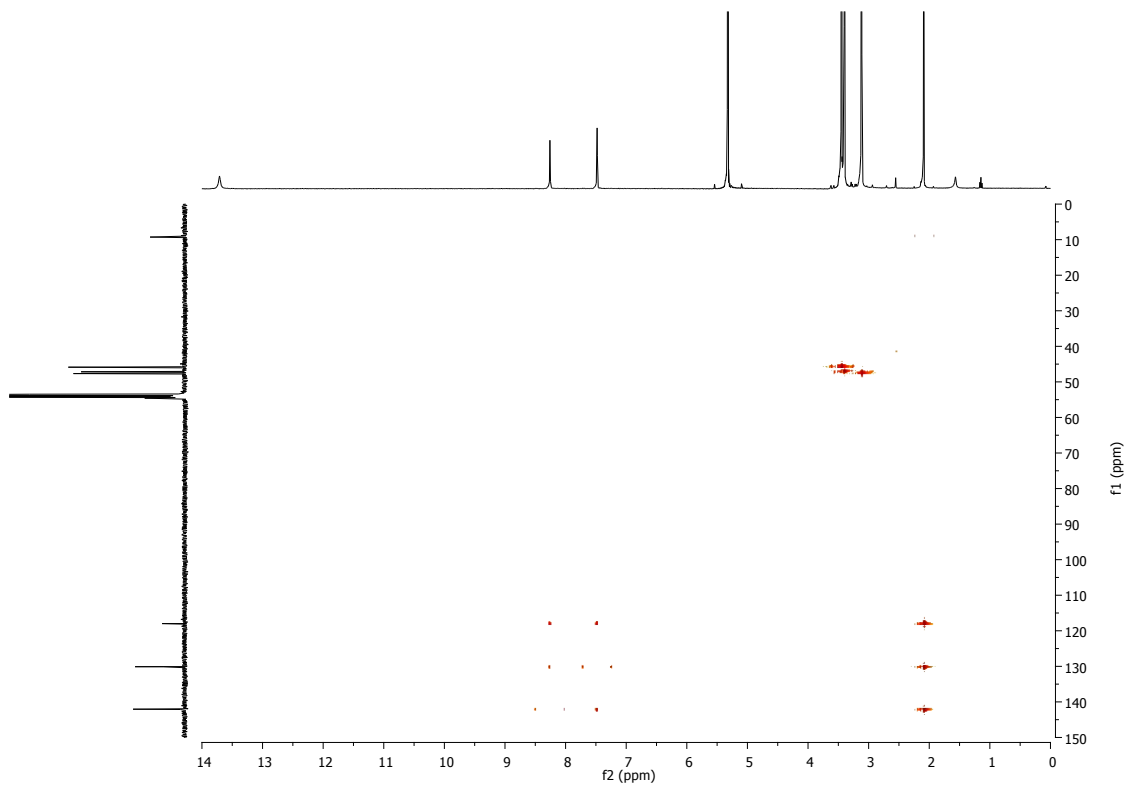
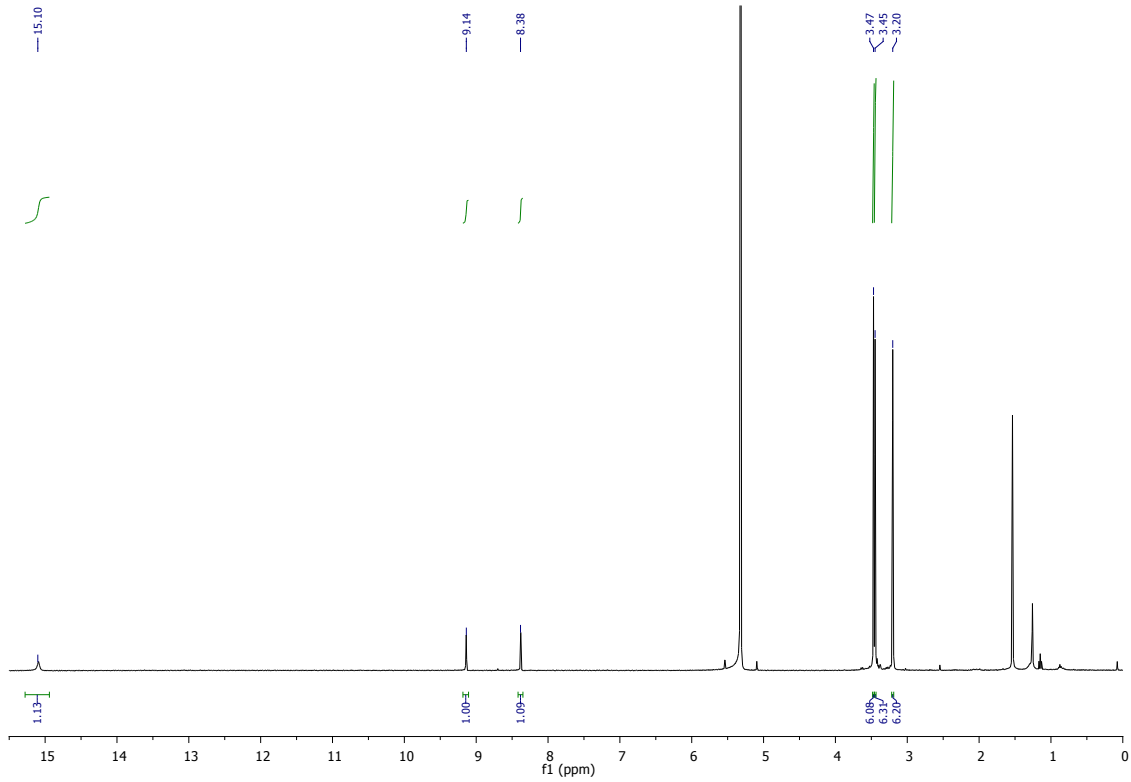
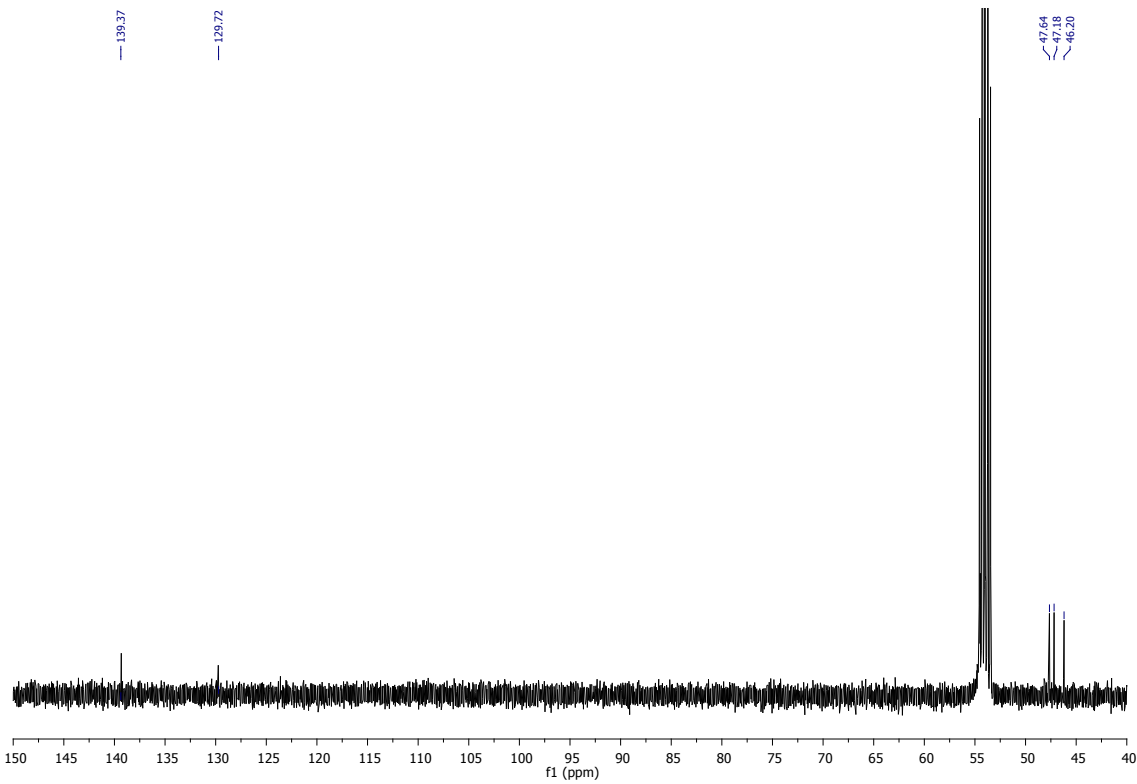


Figure S2. NMR spectra of **3**, 300 MHz, CD₂Cl₂: a) ¹H-NMR; b) ¹³C-NMR; c) COSY; d) NOESY; e) ¹H-¹³C HSQC, f) ¹H-¹³C HMBC

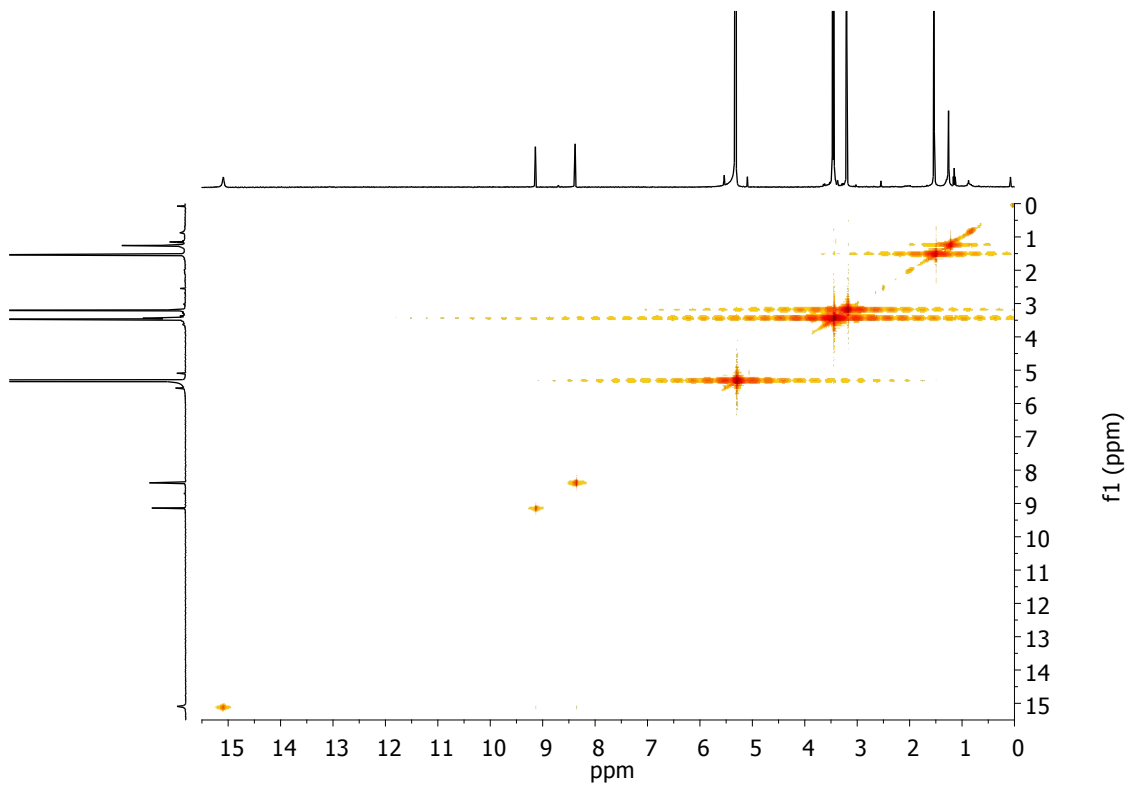
a)



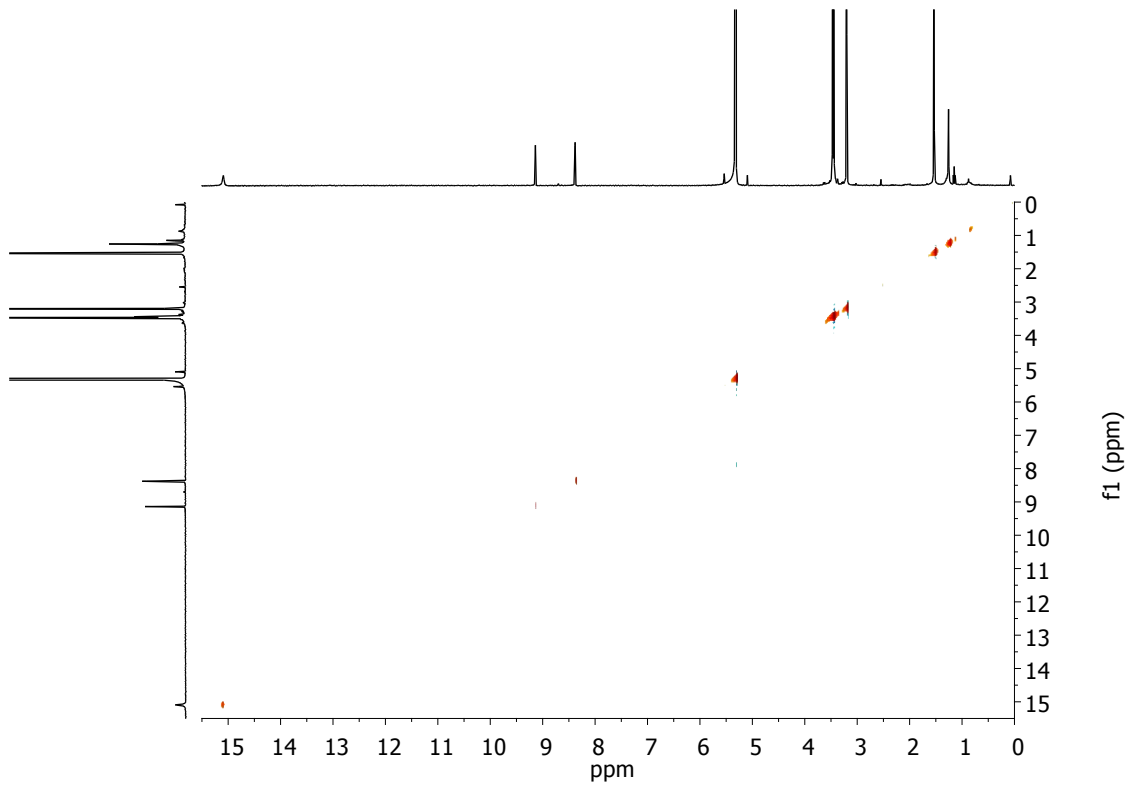
b)



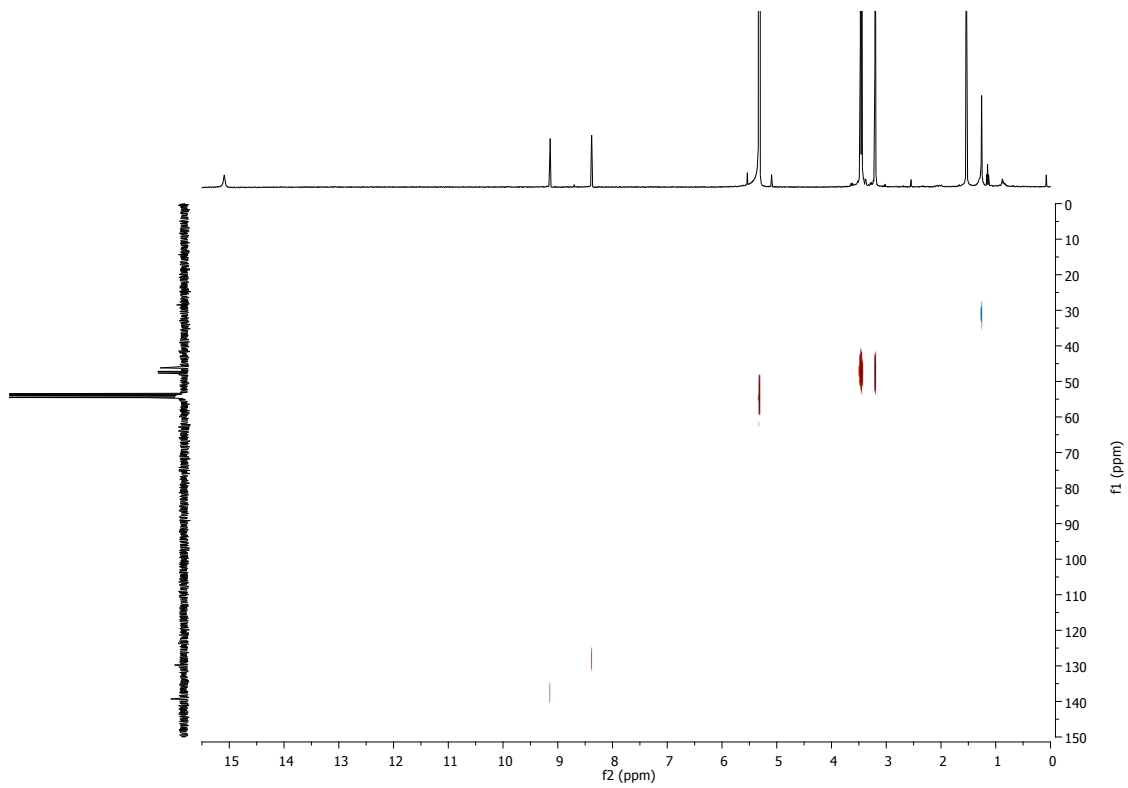
c)



d)



e)



f)

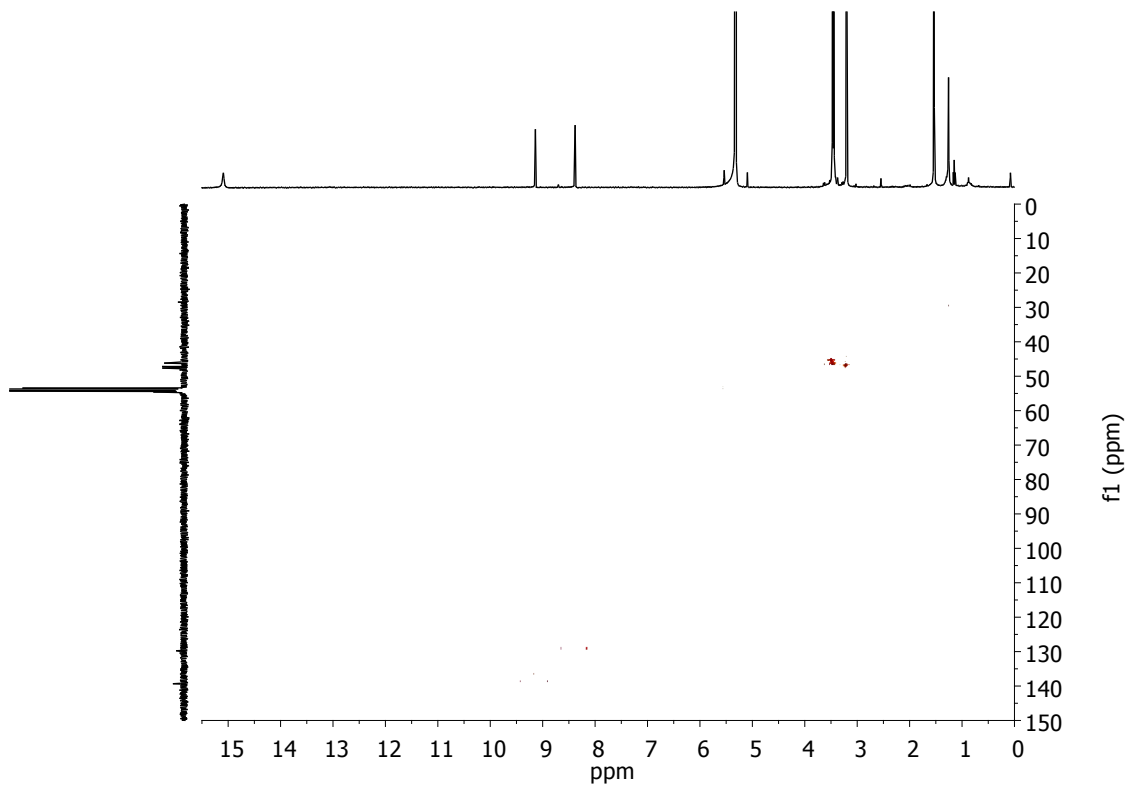
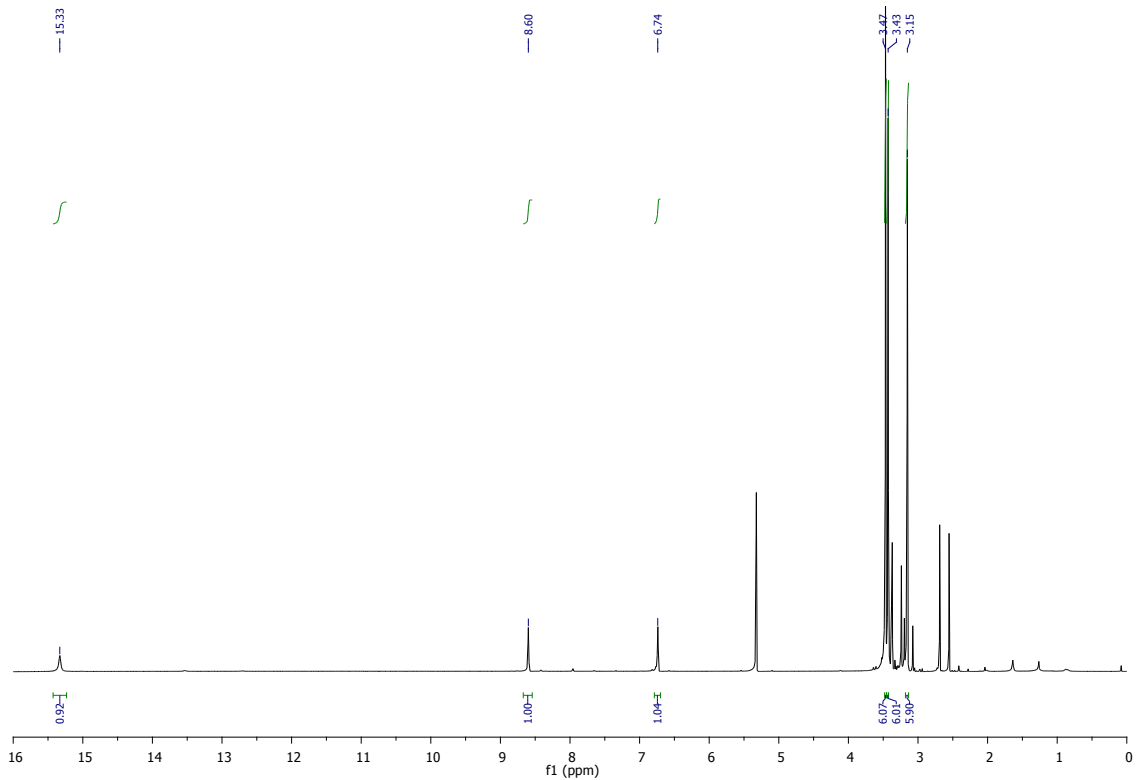
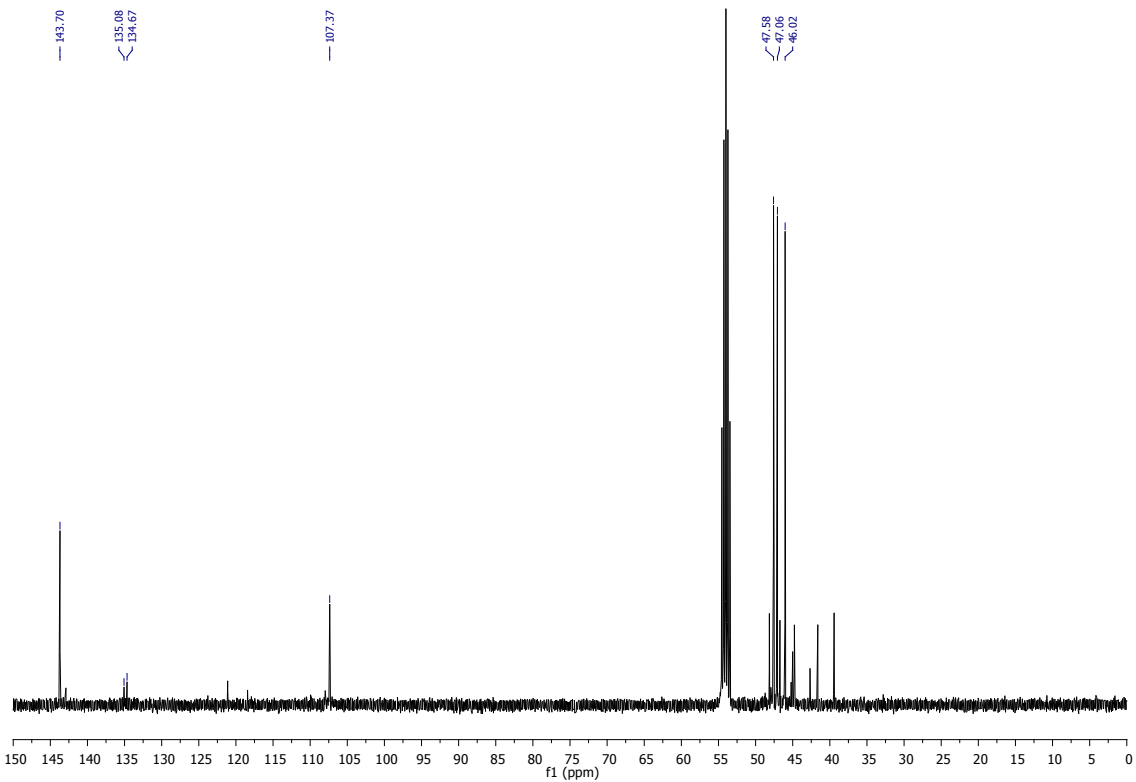


Figure S3. NMR spectra of **4**, 300 MHz, CD₂Cl₂: a) ¹H-NMR; b) ¹³C-NMR; c) COSY; d) NOESY; e) ¹H-¹³C HSQC, f) ¹H-¹³C HMBC

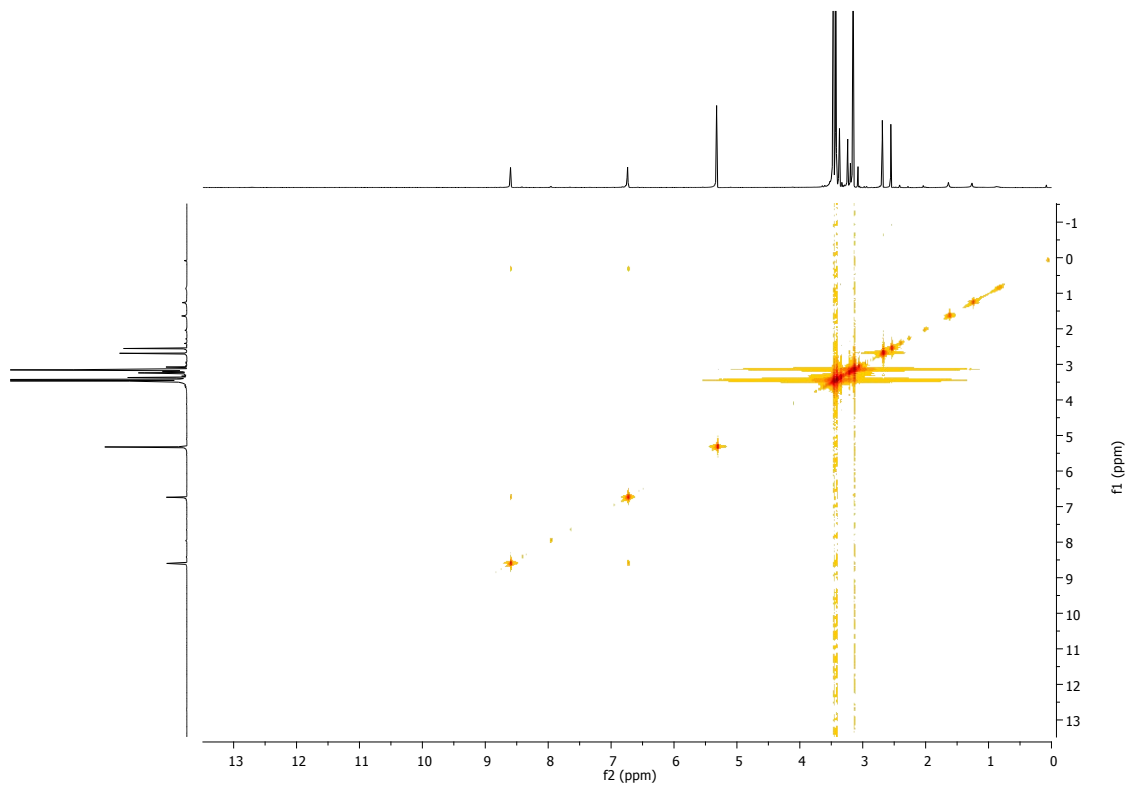
a)



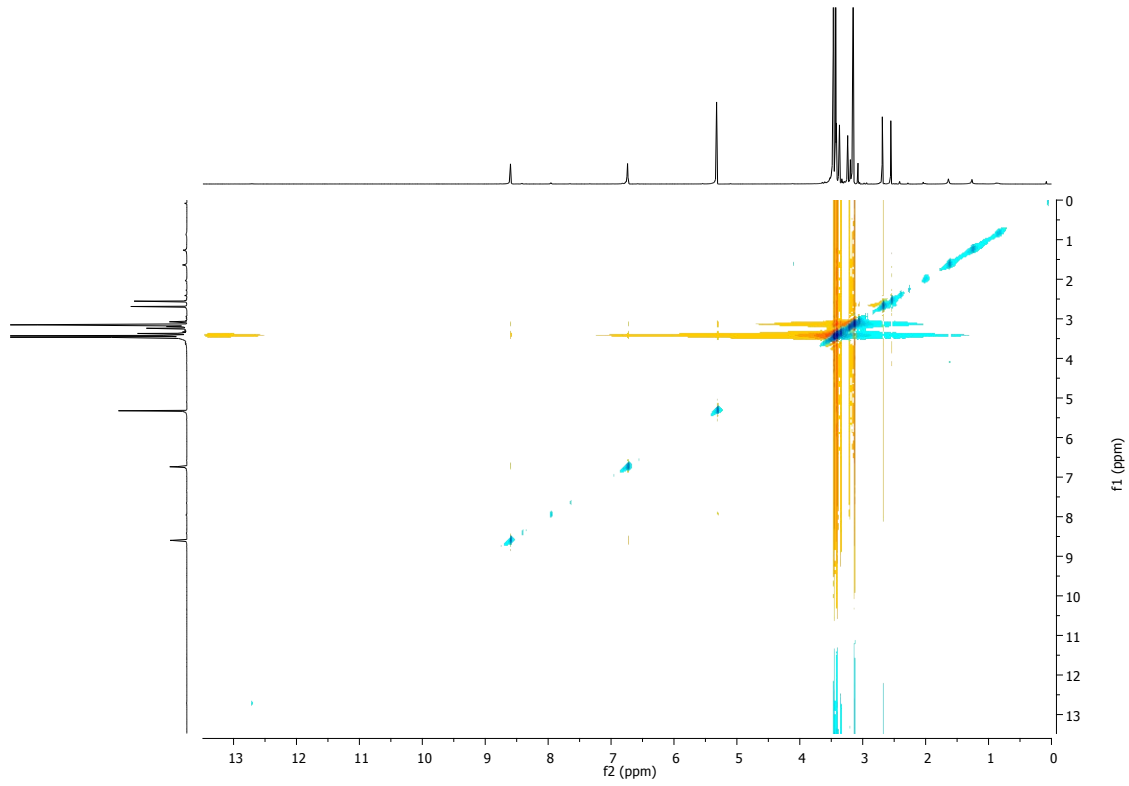
b)



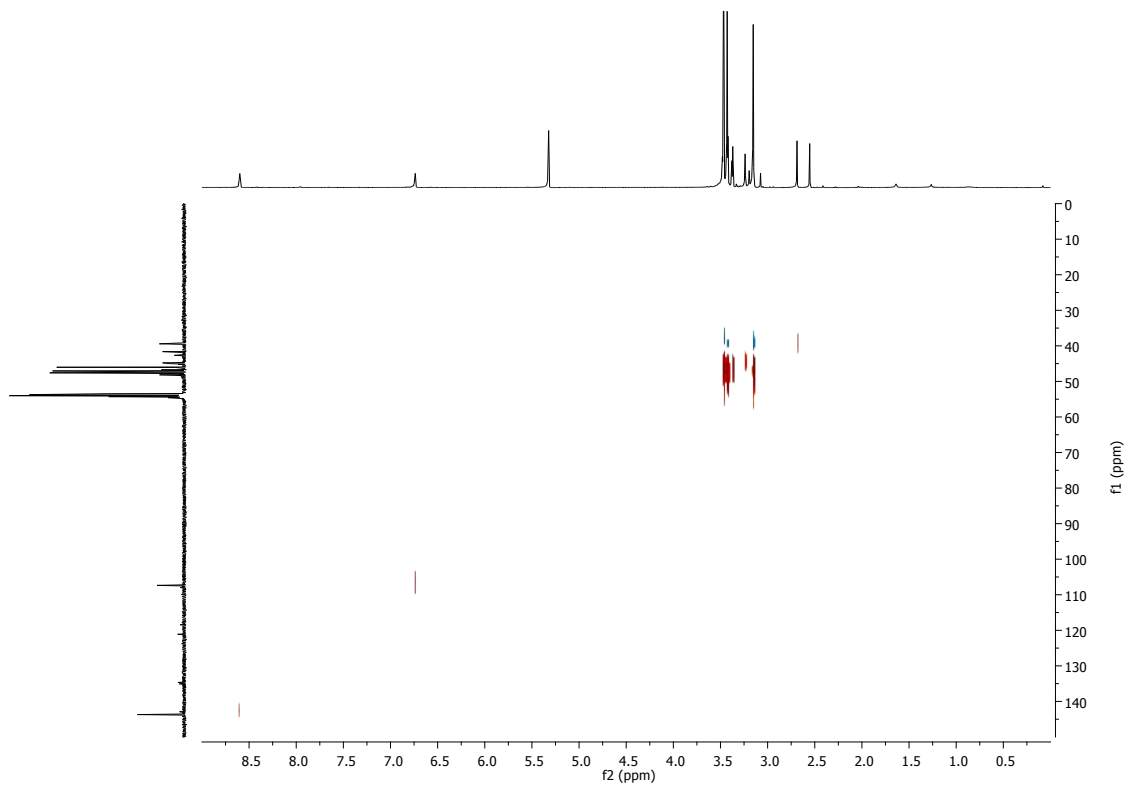
c)



d)



e)



f)

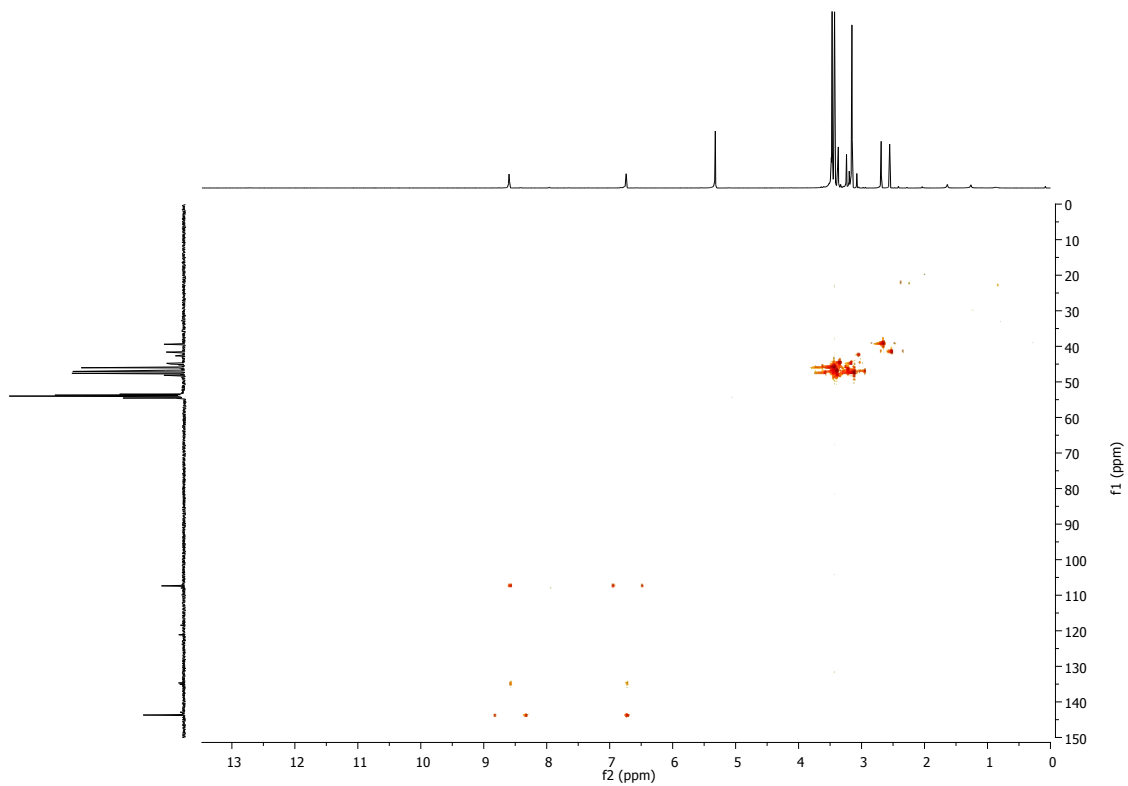
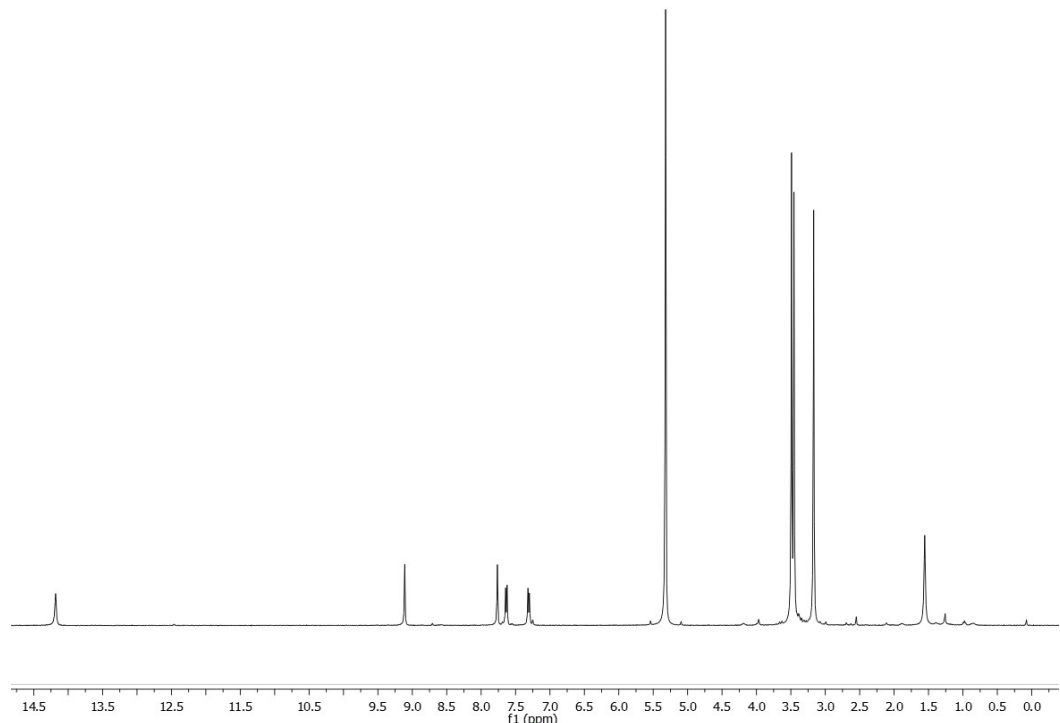
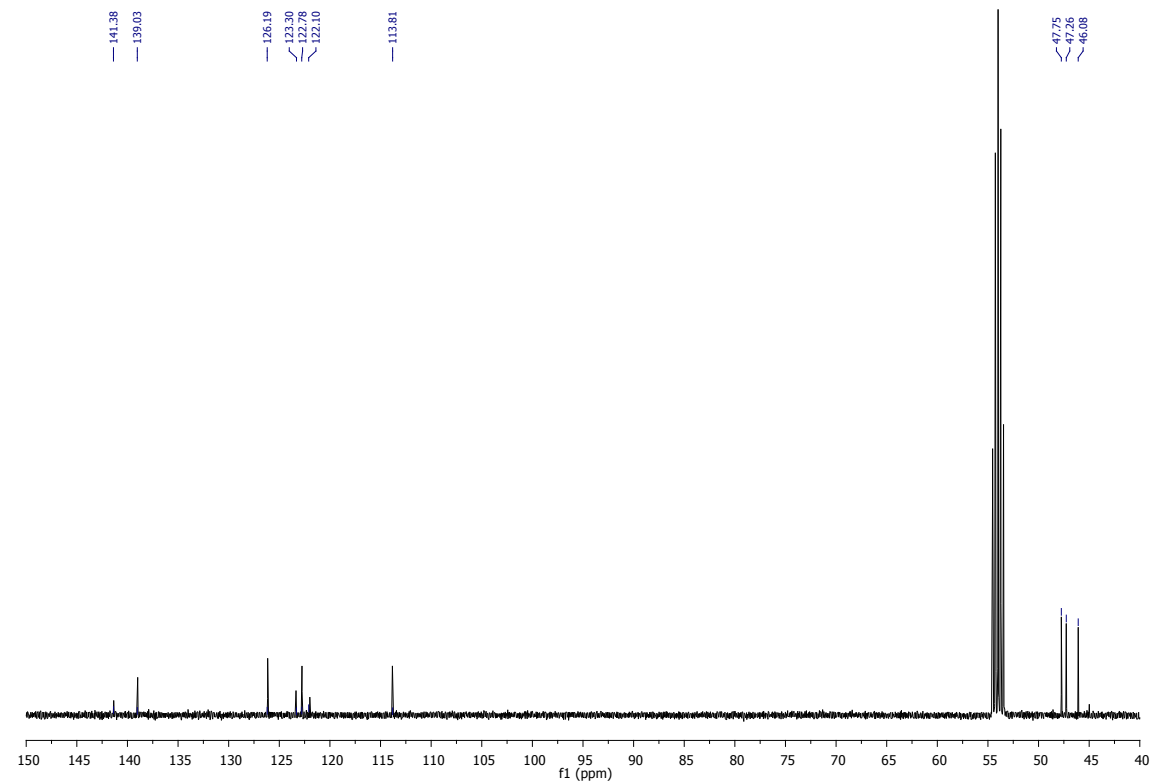


Figure S4. NMR spectra of **5**, 300 MHz, CD₂Cl₂: a) ¹H-NMR; b) ¹³C-NMR; c) COSY; d) NOESY; e) ¹H-¹³C HSQC, f) ¹H-¹³C HMBC, g) ¹H-NMR with presence of the minor isomer.

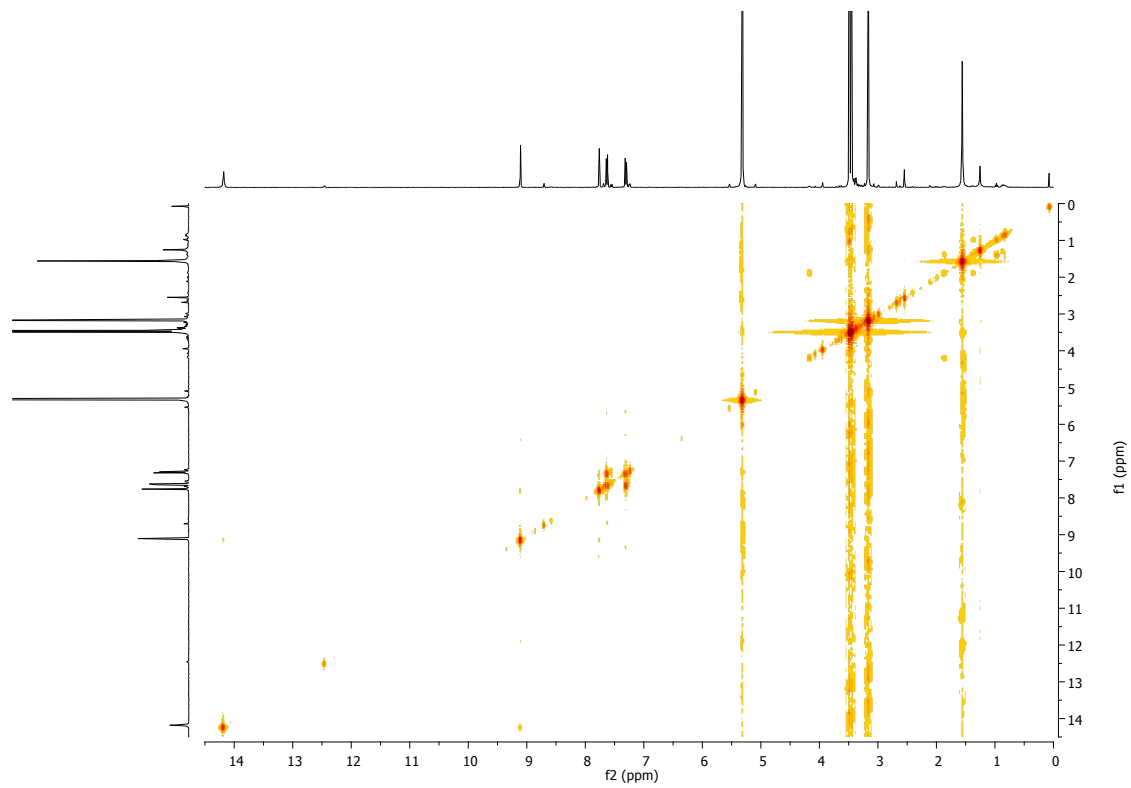
a)



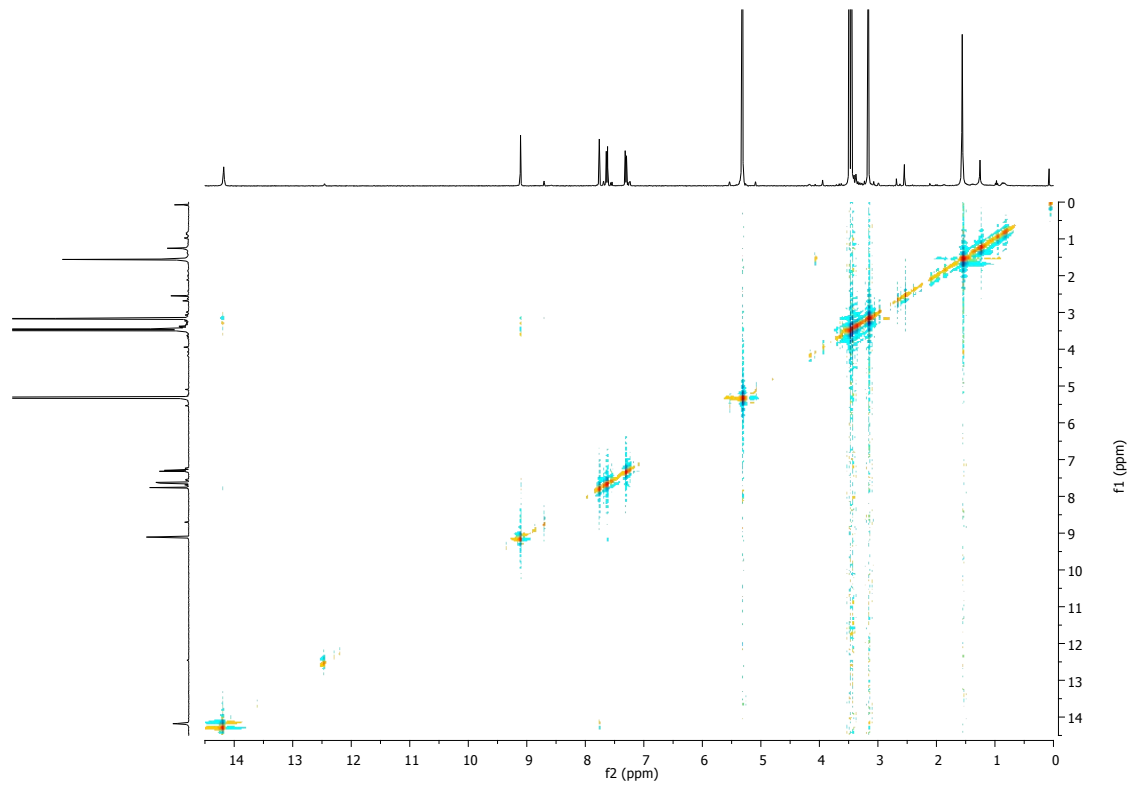
b)



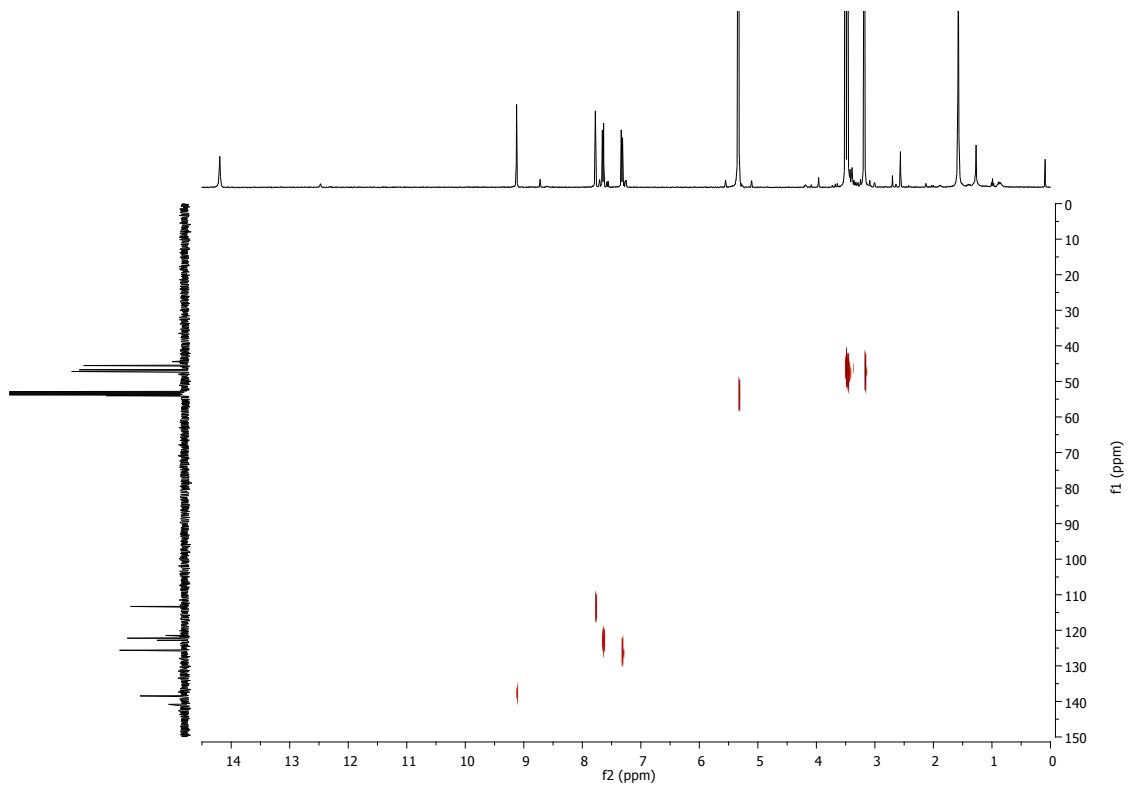
c)



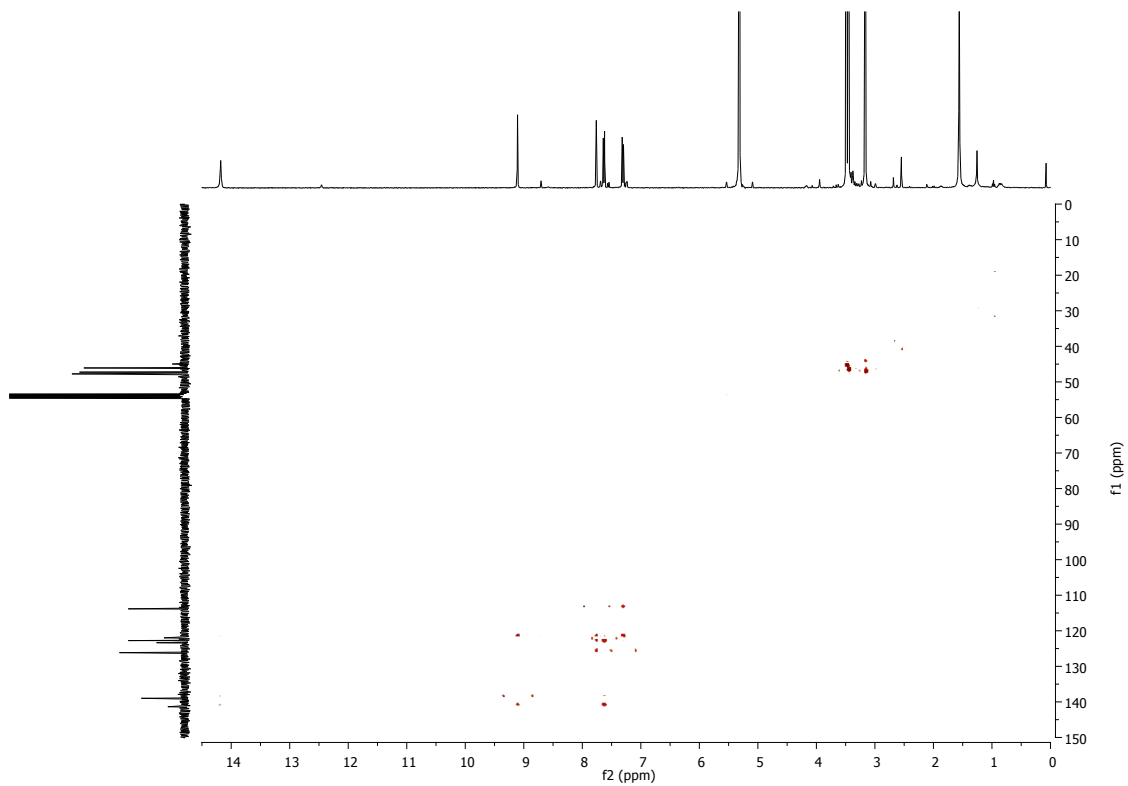
d)



e)



f)



g)

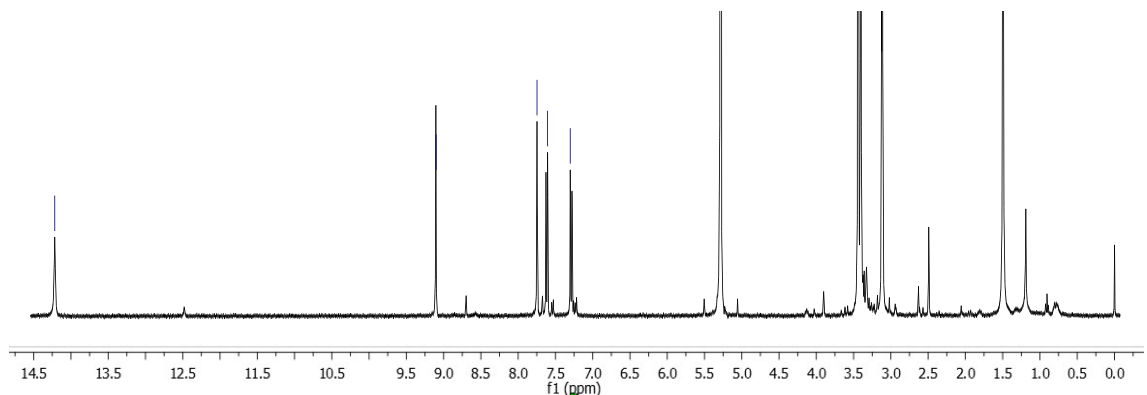


Figure S5. UV-visible spectra of **2** (blue), **3** (green), **4** (grey) and **5** (red) in CH_2Cl_2

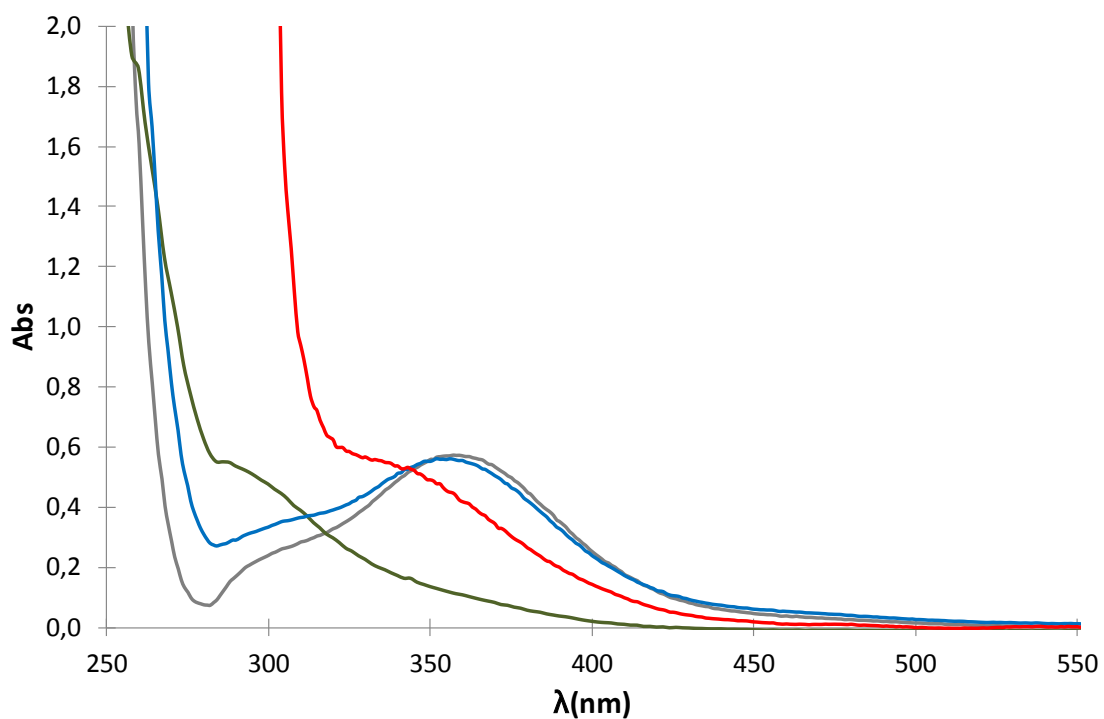


Figure S6. CV of a) **3** (blue), **4** (black) and **5** (orange) in $\text{CH}_3\text{CN} + 0.1 \text{ M TBAH}$.

a)

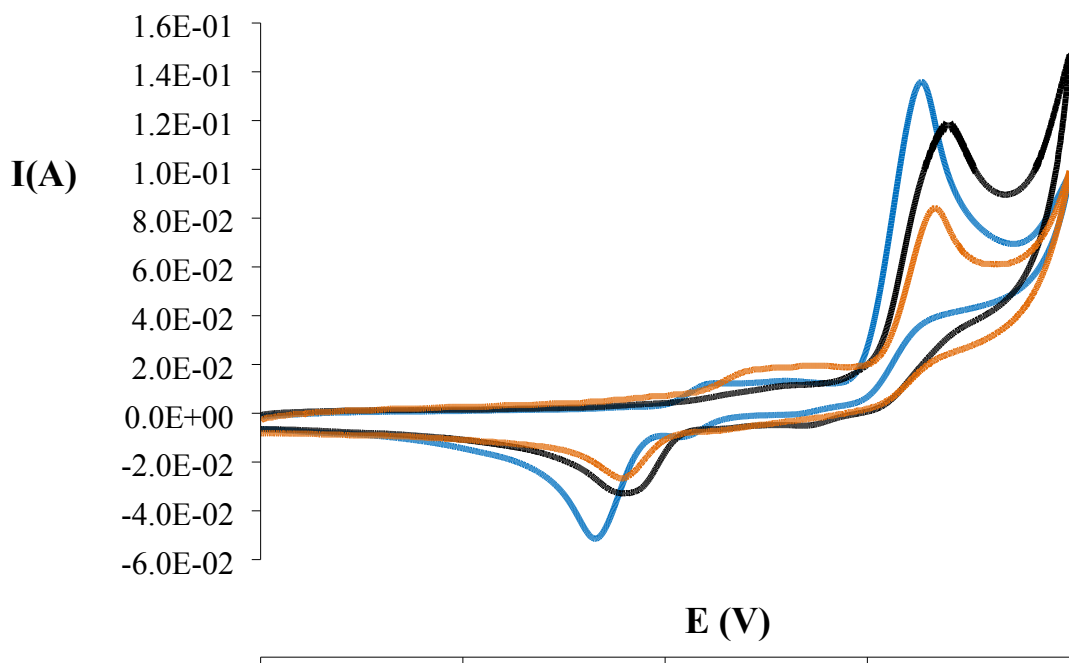


Figure S7. CV registered in CH_2Cl_2 (TBAH, 0.1M) vs Ag/AgCl starting the scanning potential at $E_{\text{init}} = 0.6$ for **2** and 0 V for **6** at scan rates between 0.20 and 8 V/s (equilibration time = 2 s).
 a) complex **2**, b) complex **6**.

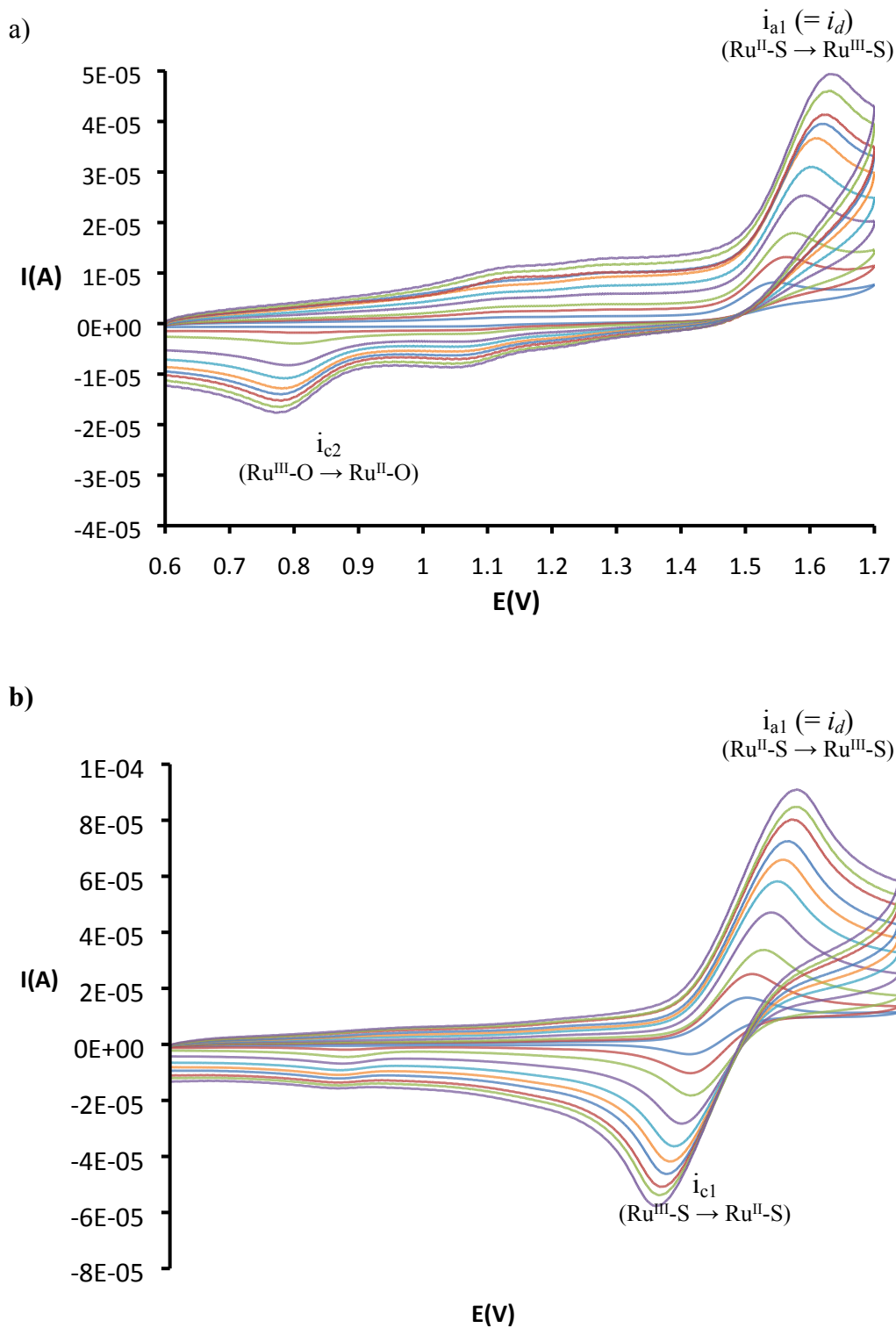


Figure S8. Plot of i_{C1}/i_{C2} vs. $1/\nu$ to obtain K^{III}_{O-S} for complex **2**.

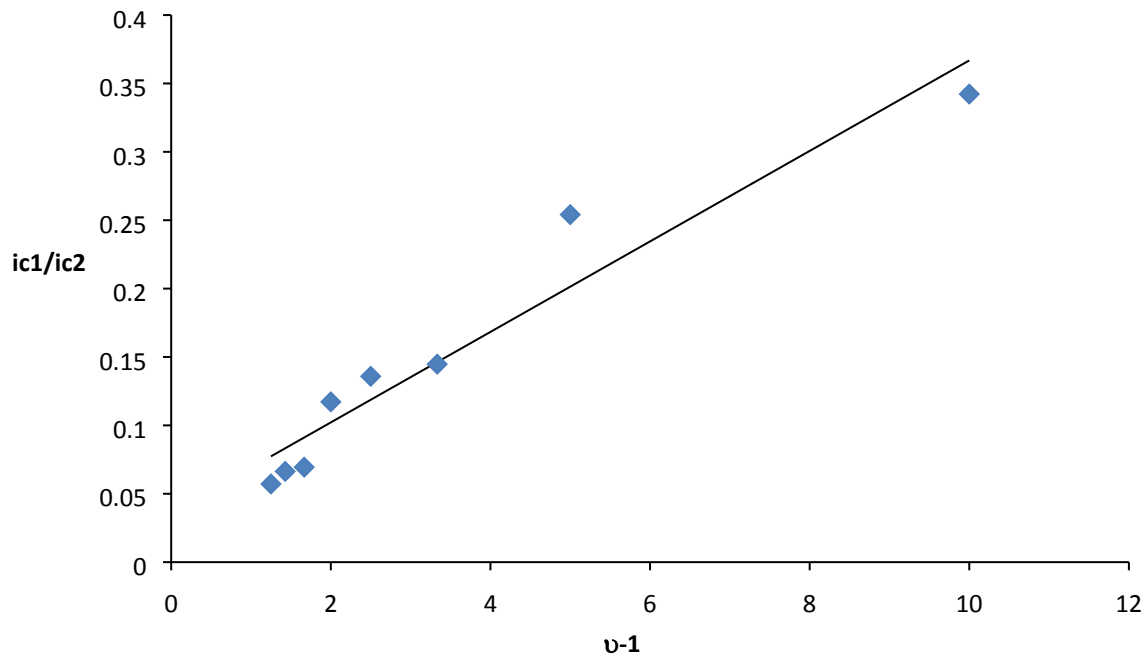


Figure S9. Plot of i_{C1}/i_{C2} vs. $1/\nu$ to obtain K^{III}_{O-S} for complex **6**.

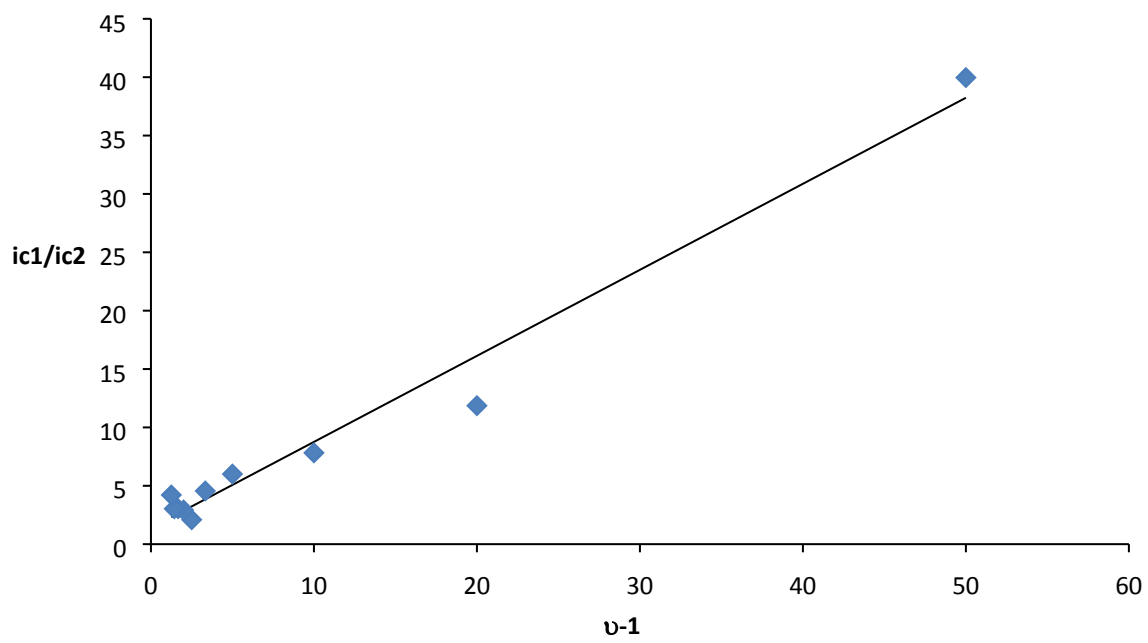


Figure S10. Plot of $v^{1/2}$ vs. i_d/i_k to obtain $k^{\text{III}}_{\text{S} \rightarrow \text{O}}$ and $k^{\text{III}}_{\text{O} \rightarrow \text{S}}$ for complex **2**.

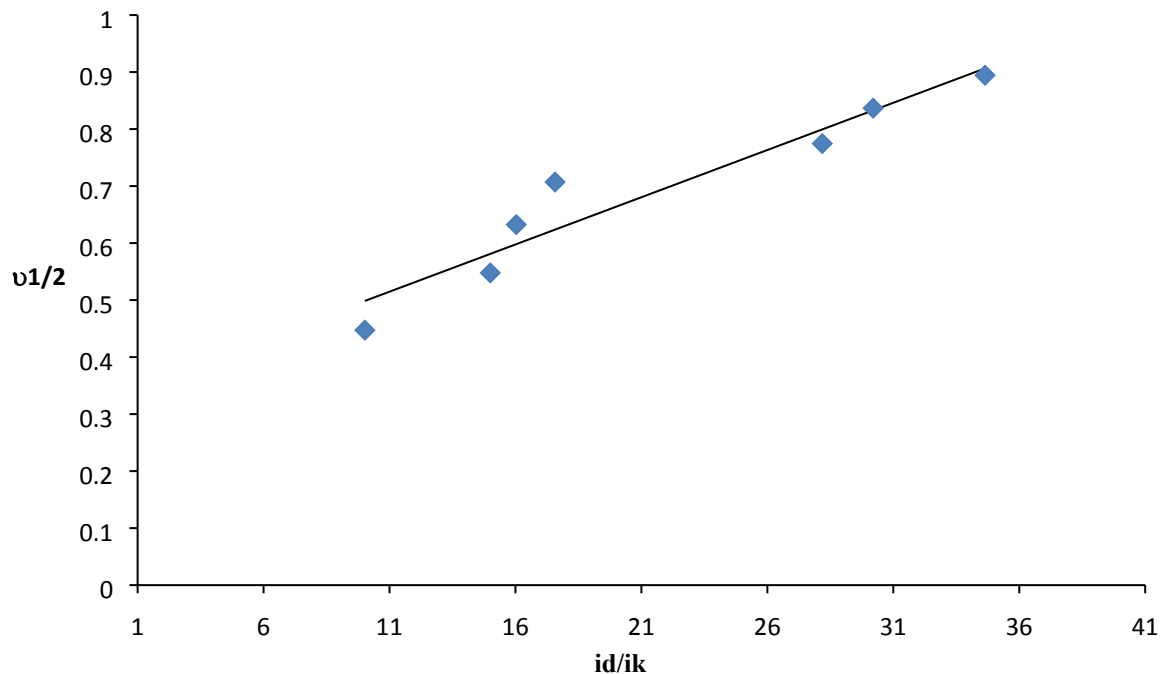


Figure S11. Plot of $v^{1/2}$ vs. i_d/i_k to obtain $k^{\text{III}}_{\text{S} \rightarrow \text{O}}$ and $k^{\text{III}}_{\text{O} \rightarrow \text{S}}$ for complex **6**.

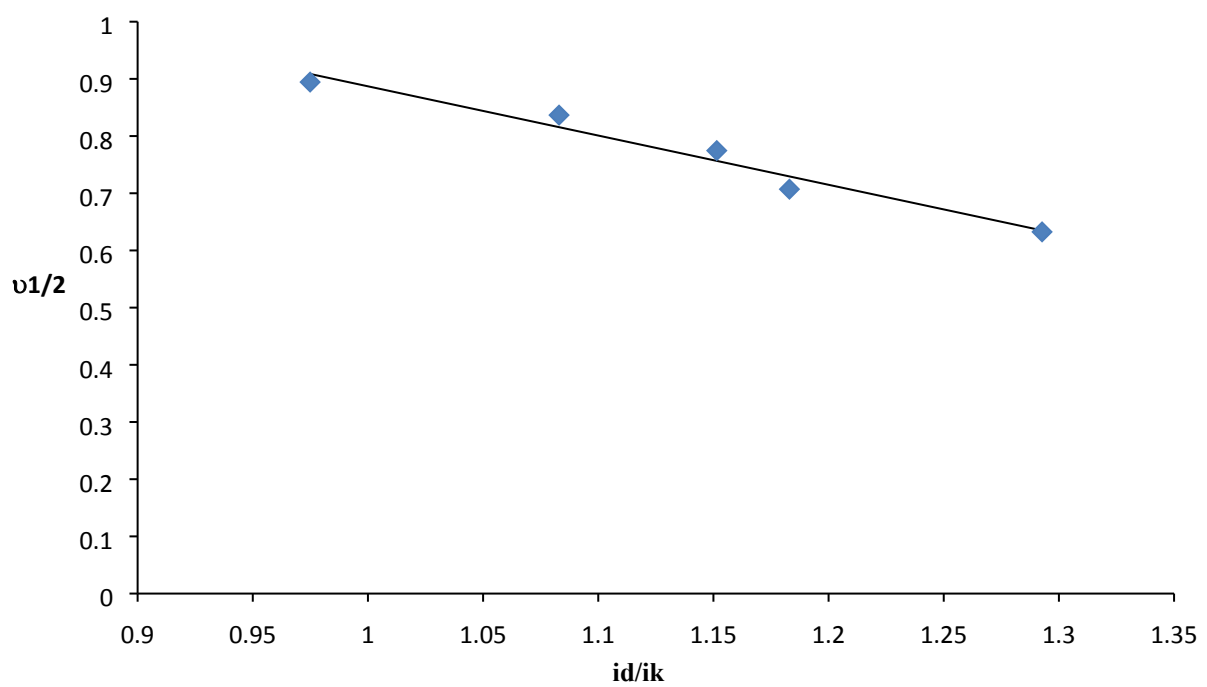


Figure S12. Plot of $\ln(i_{a1}/\nu^{1/2})$ vs. $1/\nu$ to obtain $k^{\text{II}}_{\text{O} \rightarrow \text{S}}$ for complex 2

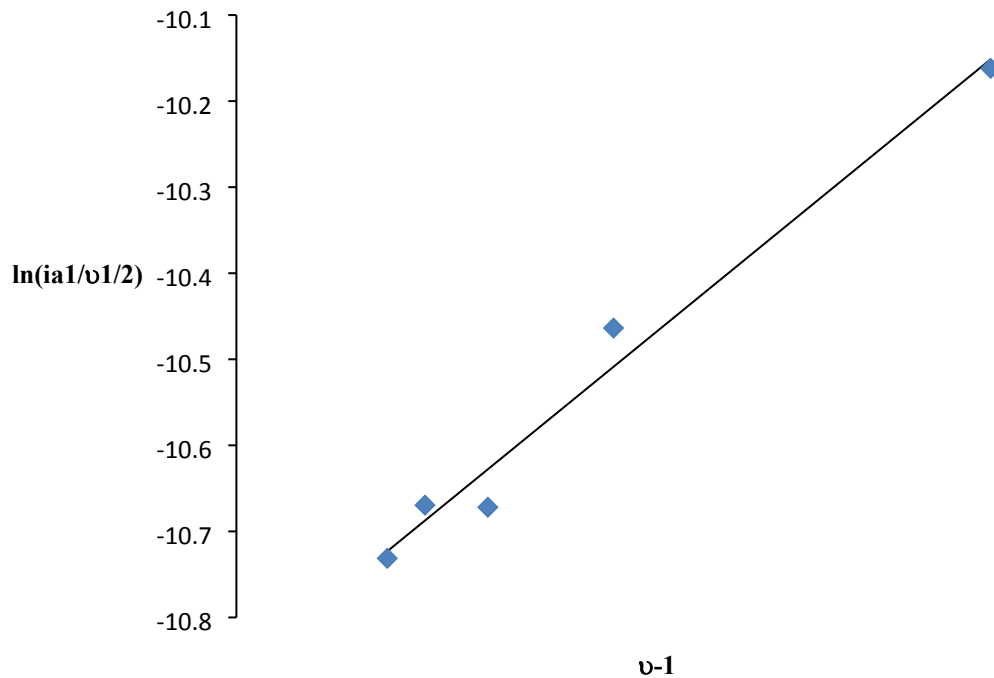


Figure S13. Plot of $\ln(i_{a1}/\nu^{1/2})$ vs. $1/\nu$ to obtain $k^{\text{II}}_{\text{O} \rightarrow \text{S}}$ for complex 6

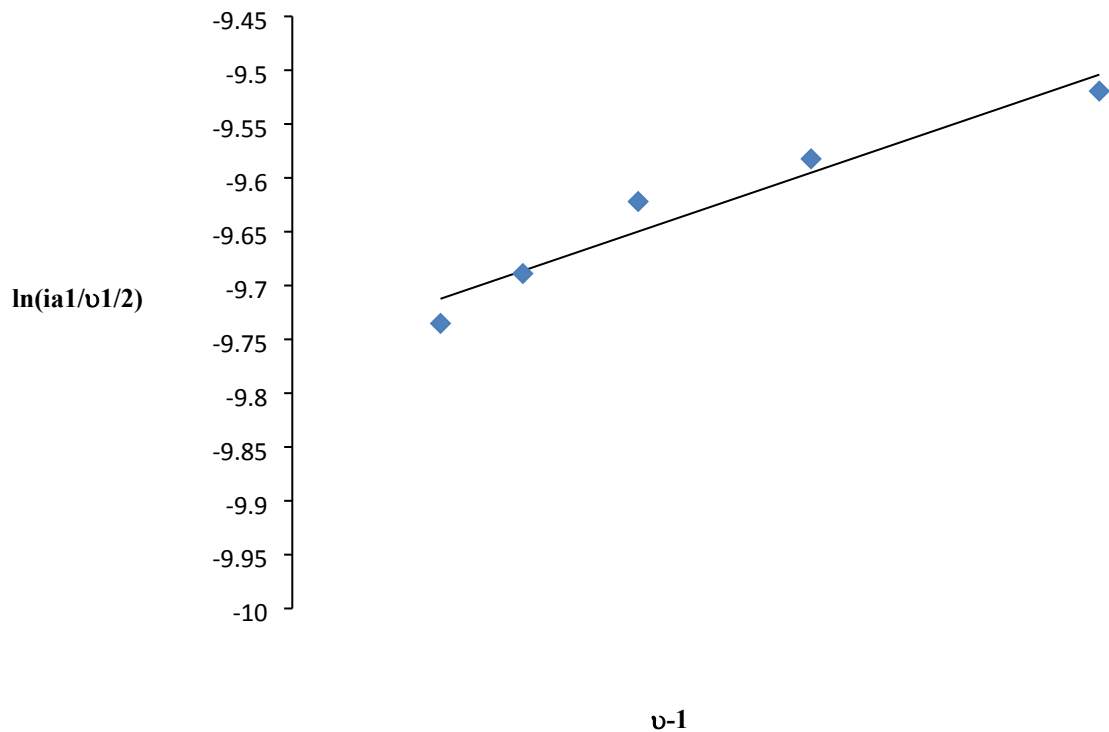


Figure S14. NMR spectra of **2** in CH₃CN after irradiation at t = a) 0, b) 45 and c) 90 minutes.

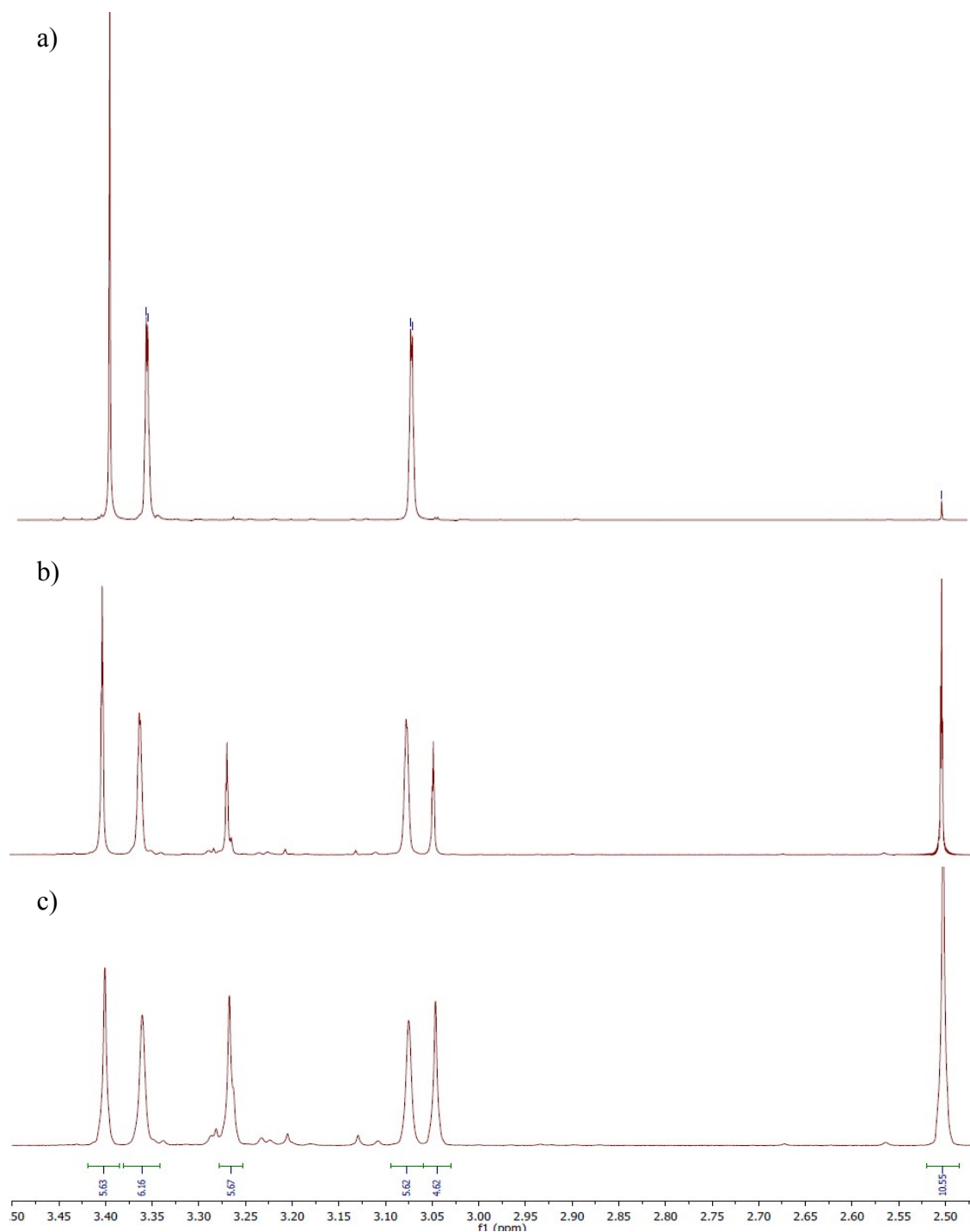


Figure S15. CV of **2** in $\text{CH}_3\text{CN} + 0.1 \text{ M TBAH}$ after irradiation during 90 minutes.

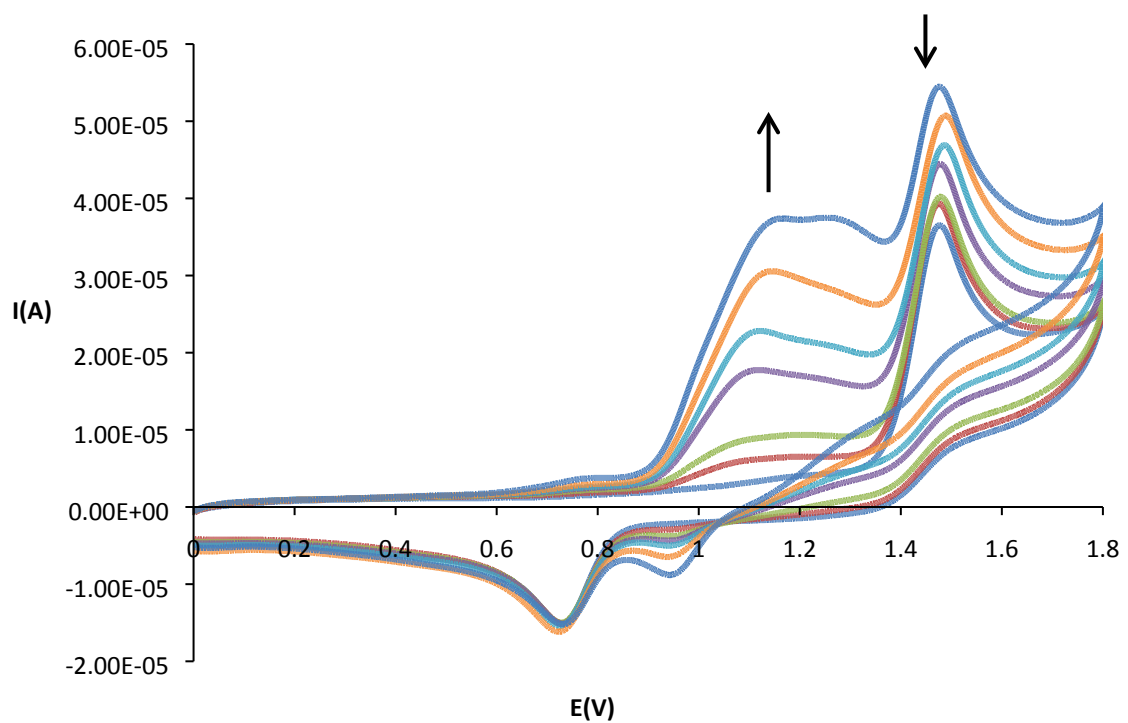


Figure S16. CV of **6'** in $\text{CH}_2\text{Cl}_2 + 0.1 \text{ M TBAH}$.

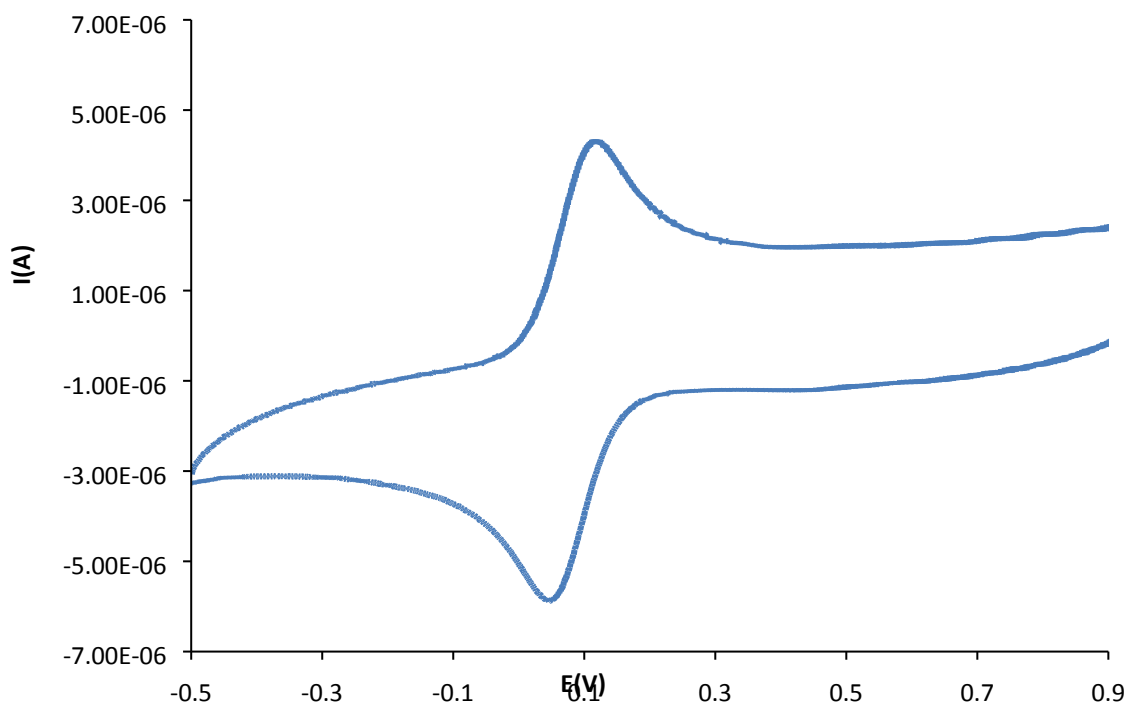


Figure S17. Successive UV-visible spectra obtained after irradiation of a solution of complex **6** in CHCl_3 during 60 min, to generate complex **6'**.

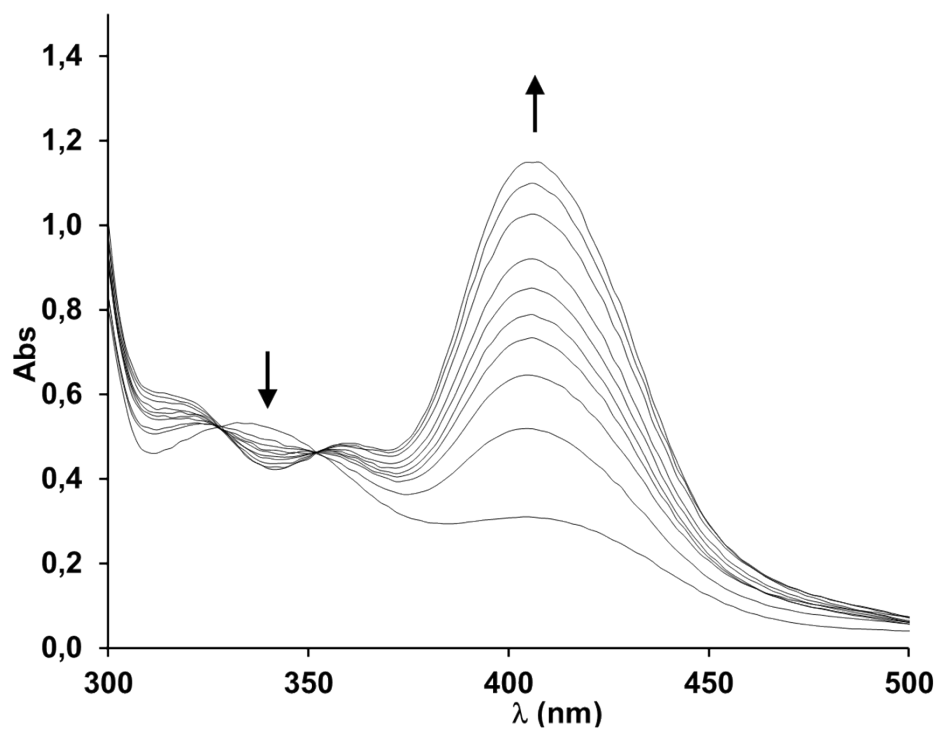


Figure S18. Successive UV-visible spectra obtained after irradiation of a solution of complex **2** in CHCl_3 during 24 h, to generate complex **2''**.

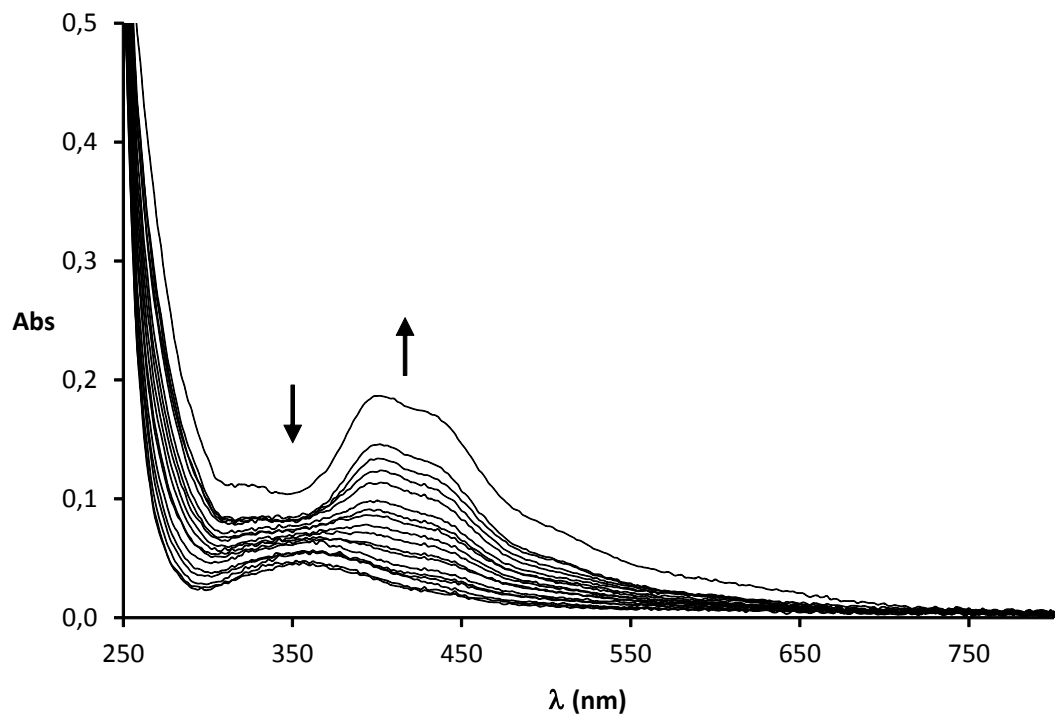


Figure S19. CV of **2''** in $\text{CH}_2\text{Cl}_2 + 0.1 \text{ M TBAH}$ after irradiation.

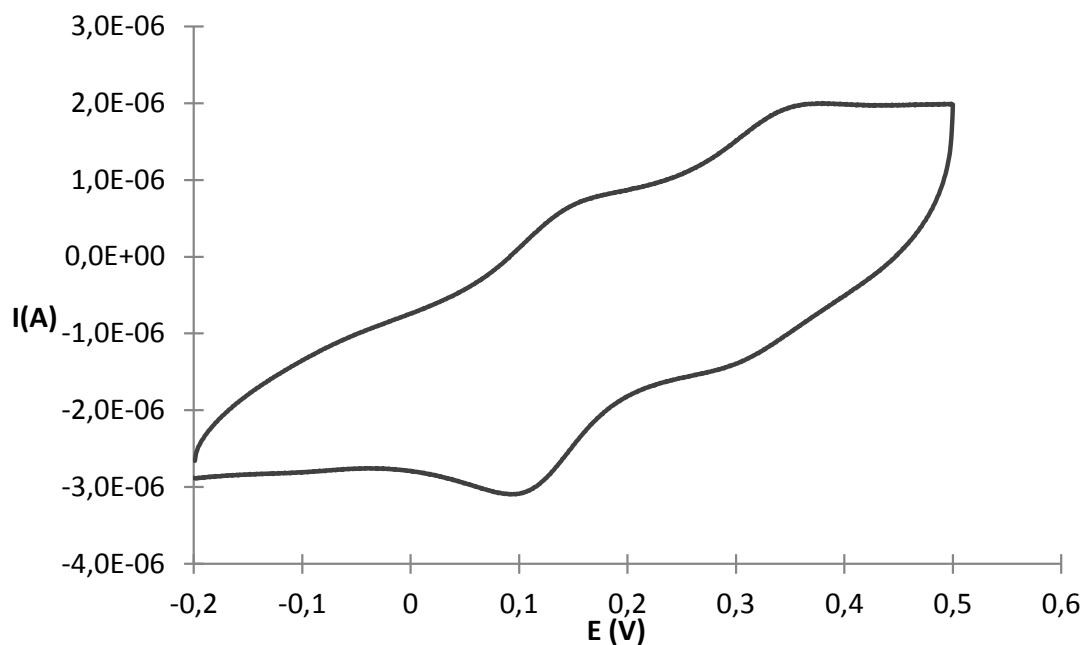


Figure S20. UV-vis monitoring of complex **2** in water at 80°C: main figure, spectra registered for 30 minutes; inset, evolution of the band at 516 nm up to 150 minutes.

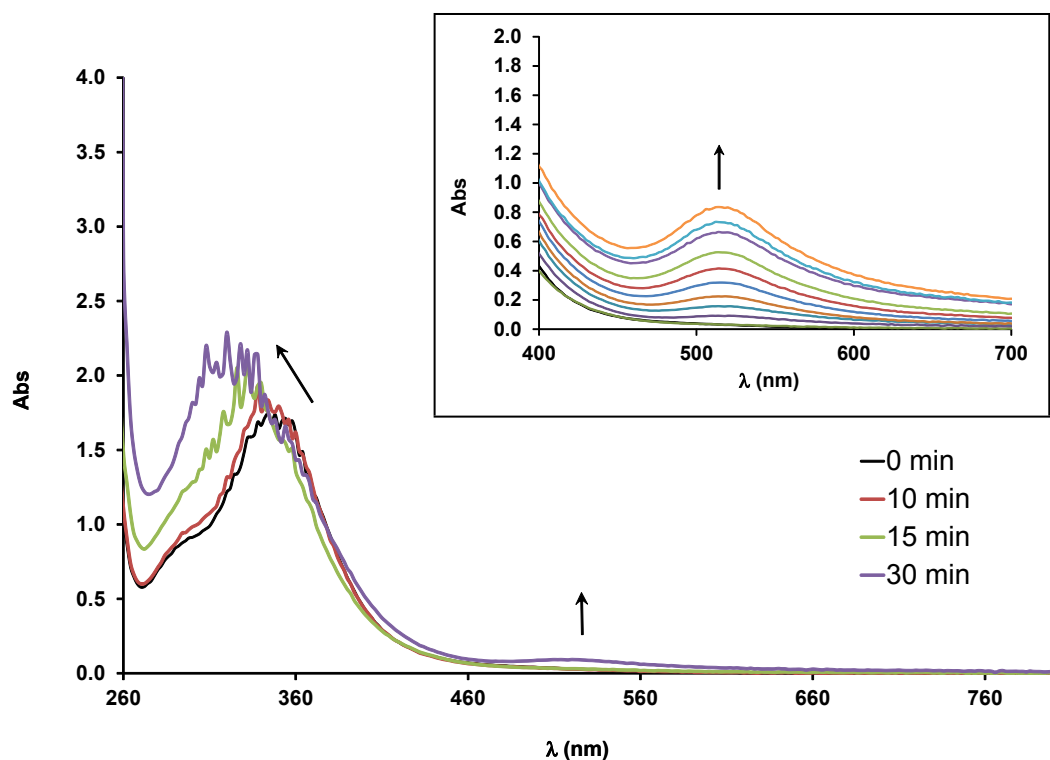


Figure S21. Red, ^1H -NMR spectrum of complex **2** registered in D_2O . Black, ^1H -NMR spectrum of complex **2** after 150 minutes in water solution at 80°C.

